Joint Time Synchronization and Localization of an Unknown Node in Wireless Sensor Networks

Jun Zheng and Yik-Chung Wu

***Abstract*—Time synchronization and localization are two important issues in wireless sensor networks. Although these two problems share many aspects in common, they are traditionally treated separately. In this paper, we present a unified framework to jointly solve time synchronization and localization problems at the same time. Furthermore, since the accuracy of synchronization and localization is very sensitive to the accuracy of anchor timings and locations, the joint time synchronization and localization problem with inaccurate anchors is also considered in this paper. For the case with accurate anchors, the joint maximum likelihood estimator and a more computationally efficient least squares (LS) estimator are proposed. When the anchor timings and locations are inaccurate, a generalized total least squares (GTLS) scheme is proposed. Cramér–Rao lower bounds (CRLBs) and the analytical mean square error (MSE) expressions of the LS based estimators are derived for both accurate and inaccurate anchor cases. Results show that the proposed joint estimators exhibit performances close to their respective CRLBs and outperform the separate time synchronization and localization approach. Furthermore, the derived analytical MSE expressions predict the performances of the proposed joint estimators very well.**

***Index Terms*—Anchor uncertainties, constrained weighted least squares, generalized total least squares, localization, maximum likelihood, time synchronization.**

I. Introduction

THE rapid advances in micro-electro-mechanical systems make it possible to produce a large number of low-cost, low-power and multi-functional tiny sensor nodes, and thus propels the implementation of modern large scale wireless sensor networks (WSNs). Because of its wide applications in environmental monitoring, natural disaster prediction, health care, manufacturing and transportation, WSNs have attracted enormous interests in recent years [1], [2].

In WSNs, synchronization supports functions such as time-based channel sharing, power scheduling, and time-based localization in WSNs. Various time synchronization methods have been developed specifically for WSNs in the literature. The most prominent methods are Reference Broadcast Synchronization [6], Timing-sync Protocol for Sensor Networks (TPSN) [7], and Flooding Time Synchronization Protocol (FTSP) [8]. Recently, Noh *et al.* mathematically evaluated the performances of time synchronization methods based on two-way message exchange [9].

On the other hand, localization is the basis of applications which require accurate locations of the sensor nodes, such as target and event tracking, emergency rescue and geographic routing [1]. Among the current localization techniques, the most accurate localization approaches are anchor and range based methods. These methods usually use the time-of-arrival (TOA), time-difference-of-arrival (TDOA) or received signal strength (RSS) to compute the distances between nodes and anchors, and then obtain locations of the nodes from the calculated distances [3]–[5].

Traditionally, synchronization is mainly studied from protocol design of view [10], while localization is studied from the signal processing point of view [3], [4]. As a result, these two problems have been investigated separately for a long time. However, the fact is that synchronization and localization have very close relationships and share many aspects in common. Furthermore, the accuracy of the time synchronization is a central issue in time-based localization approaches, such as the TOA based Two-way Ranging scheme in IEEE 802.15.4a standard [21]. As will be shown in the simulation results of this paper, time-based localization cannot provide accurate location estimates under inaccurate timings.

Based on the close relationships between time synchronization and localization, it is natural to explore the possibility of formulating them into a unified framework and solve the two problems at the same time. Recently, some pioneering research works noticed the similarities between the problem of time synchronization and localization [12], [13]. However, they only pointed out the links between the two problems and explored the possibility of jointly implementing time synchronization and localization in protocol level. Denis *et al.* took a step further in [14] by solving the two problems together in the physical layer. Unfortunately, strictly speaking, [14] cannot be categorized as joint approach since time synchronization is performed first and localization is carried out based on the synchronization results. In this paper, we propose a unified framework to jointly synchronize the unknown nodes and locate them to the anchors simultaneously. In particular, in the first half of the paper, where the anchors' timing and location information is assumed to be accurate, the maximum likelihood (ML) estimator and a low-complexity least squares (LS) based estimator are derived.

In WSNs, hierarchical method is usually used to synchronize and localize a large sensor field. Some sensor nodes are synchronized and localized to the anchors first, and then they become new anchors and are used to synchronize and localize other

Manuscript received December 18, 2008; accepted September 01, 2009. First published September 25, 2009; current version published February 10, 2010. The associate editor coordinating the review of this manuscript and approving it for publication was Dr. Zhi Tian.

The authors are with the Department of Electrical and Electronic Engineering, The University of Hong Kong, Hong Kong (e-mail: zhengjun@eee.hku.hk; ycwu@eee.hku.hk).

Color versions of one or more of the figures in this paper are available online at http://ieeexplore.ieee.org.

Digital Object Identifier 10.1109/TSP.2009.2032990

nodes. This procedure is repeated until all nodes are synchronized and localized [7], [15]. Unfortunately, this hierarchical synchronization and localization method results in error propagation due to the inaccuracy of estimations at each level. In this case, taking the uncertainties of anchor timing and location into account is important for error propagation relief. Ho *et al.* considered the anchor errors in the scenario of localization [16]. However, there is no reported work considering anchor error in time synchronization. In the second half of the paper, both the timing and location uncertainties of anchors are incorporated in the system model, and a novel estimator is proposed based on the generalized total least squares (GTLS) method. Notice that the hierarchical time synchronization and localization method we consider in this paper is a centralized approach in the sense that the procedure starts from the anchors and proceeds to the next level. It is different from many distributed time synchronization techniques, such as clock consensus and gossip averaging, where no reference node is needed [17]–[19].

In addition to estimator derivations, the performances of the proposed algorithms are also analyzed in this paper. The Cramér–Rao lower bounds (CRLBs) are derived for both cases with accurate and inaccurate anchor information. Furthermore, analytical mean square error (MSE) expressions are derived for the two proposed LS based schemes.

The rest of the paper is organized as follows. The system model is introduced in Section II, followed by the ML estimator and the proposed low-complexity estimator in Section III. Joint time synchronization and localization with anchor uncertainties is discussed in Section IV. The CRLBs and MSE performances of the proposed estimators are derived in Section V. In Section VI, simulation results are presented. Finally, conclusions are drawn in Section VII.

Notations: The following notations are used in this paper. The special matrices $\mathbf{1}_{M\times N}, \mathbf{0}_{M\times N}, \boldsymbol{I}$ and $\boldsymbol{E}_{M\times 1}$ denote the $M\times N$ matrix of ones, $M\times N$ matrix of zeros, identity matrix, and $M\times 1$ vector of alternating -1 and 1, respectively. The operators $\otimes$, $\odot$, $\mathrm{Tr}(\cdot)$ and $\{\cdot\}^T$ denote the Kronecker product, the Hadamard product (i.e., element by element product), the trace of a square matrix and the transpose of a matrix, respectively. The Euclidean norm of a vector and Frobenius norm of a matrix are denoted as $\|\cdot\|$ and $\|\cdot\|_F$, respectively, while $|\cdot|$ is the absolute value of a scalar or the determinant of a matrix. The operator $\mathbb{E}\{\cdot\}$ is the expectation of a random variable or matrix, $\mathrm{diag}\{\boldsymbol{A},\boldsymbol{B}\}$ is a matrix with $\boldsymbol{A}$ and $\boldsymbol{B}$ on its diagonal and all other elements zero.

II. System Model

In this paper, we consider hierarchical hop-by-hop time synchronization and localization in a sensor network, and focus our study on the scenario that only one node needs to be synchronized and localized to the anchors at a time. In the considered system, it is assumed that there are L $(L \geq 3)$ anchors with known timings and locations. The l^{th} anchor A_l is located at $\boldsymbol{a}_l^o = [a_{xl}^o, a_{yl}^o]^T$ with time skew θ_{sl}^o and time offset θ_{0l}^o. The node to be synchronized and localized is denoted as Node B with unknown location $\boldsymbol{x} = [x, y]^T$, time skew θ_s and time offset θ_0.

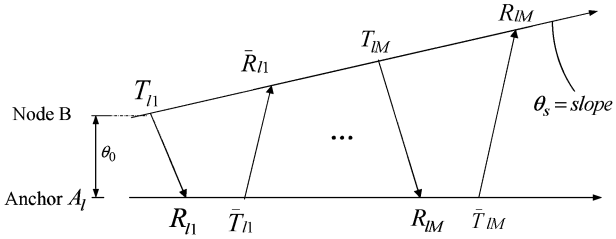

Fig. 1. Two-way time-stamp exchange between Node B and the l^{th} anchor A_l.

Node B and the anchors exchange time-stamps based on two-way message exchanges [9] as shown in Fig. 1. Assume there are M rounds of two-way message exchanges between Node B and anchor A_l. During the m^{th} round exchange, a message is sent from Node B at time T_{lm} and is received by A_l at time R_{lm}. Then, anchor A_l replies Node B with another message sent at $\bar{T}_{lm}$ and is received by Node B at $\bar{R}_{lm}$. In the reply message from anchor A_l to Node B, the received time-stamps R_{lm} and $\bar{T}_{lm}$ at the anchor side are also included. Therefore, after the m^{th} round of message exchange, Node B has all the time-stamp information $\{T_{lm}, R_{lm}, \bar{T}_{lm}, \bar{R}_{lm}\}$. Note that R_{lm} and $\bar{T}_{lm}$ are measured with respect to the clock of anchors, while T_{lm} and $\bar{R}_{lm}$ are measured with respect to the clock of Node B. In this paper, we focus on the line-of-sight (LOS) propagation between Node B and the anchors, and the exchanged time-stamps can be modeled as [20]

$$T_{lm} = \frac{\theta_s}{\theta_{sl}^o} R_{lm} - \theta_s(t_l + n_{lm}) + \theta_0 - \frac{\theta_s}{\theta_{sl}^o}\theta_{0l}^o \tag{1}$$

$$\bar{R}_{lm} = \frac{\theta_s}{\theta_{sl}^o} \bar{T}_{lm} + \theta_s(t_l + \bar{n}_{lm}) + \theta_0 - \frac{\theta_s}{\theta_{sl}^o}\theta_{0l}^o \tag{2}$$

where $t_l = \|\boldsymbol{x} - \boldsymbol{a}_l^o\|/c$ is the propagation delay between Node B and anchor A_l, with c being the speed of light. Symbols n_{lm} and $\bar{n}_{lm}$ are the TOA detection errors, which are Gaussian distributed [14]. With the impulse-radio ultra-wideband technology and physical layer time-stamping, the TOA detection errors are in the order of nanosecond (ns) [21]. The goal of joint time synchronization and localization is to estimate x, y, θ_s and θ_0 of Node B based on the observed time-stamps in (1) and (2), and the anchor locations and timing a_{xl}^o, a_{yl}^o, θ_{sl}^o and θ_{0l}^o.

III. Joint Timing and Location Estimation Algorithms

Without loss of generality, it is assumed in this section that all the L anchors are synchronized to the same reference time, and thus the time skew and time offset for all anchors are $\theta_{sl}^o = 1$ and $\theta_{0l}^o = 0$, respectively. Therefore, (1) and (2) becomes

$$T_{lm} = \theta_s(R_{lm} - t_l - n_{lm}) + \theta_0 \tag{3}$$

$$\bar{R}_{lm} = \theta_s(\bar{T}_{lm} + t_l + \bar{n}_{lm}) + \theta_0. \tag{4}$$

In this section, the ML joint timing and location estimator is first derived based on (3) and (4). However, it is found that a two-dimensional search is needed to obtain the solution for the ML estimator. In order to avoid the computationally expensive numerical search, in the second part, we propose a low-complexity two-stage LS estimator.

A. Maximum Likelihood Estimator

Dividing both sides of (3) and (4) by θ_s and introducing two new variables $\theta_1 \triangleq 1/\theta_s$ and $\theta_2 \triangleq \theta_0/\theta_s$, we have

$$-R_{lm} + t_l = -T_{lm}\theta_1 + \theta_2 - n_{lm} \tag{5}$$

$$\bar{T}_{lm} + t_l = \bar{R}_{lm}\theta_1 - \theta_2 - \bar{n}_{lm}. \tag{6}$$

Collecting all the M round of exchanged time-stamps from the l^{th} anchor, and introducing $\boldsymbol{\theta} \triangleq [\theta_1 \theta_2]^T$, we can put (5) and (6) for the l^{th} anchor A_l into a matrix form

$$\boldsymbol{T}_l(\boldsymbol{x}) = \boldsymbol{R}_l\boldsymbol{\theta} - \boldsymbol{n}_l \tag{7}$$

where $\boldsymbol{T}_l(\boldsymbol{x}) = \boldsymbol{T}_{al} + t_l\mathbf{1}_{2M\times 1}$, $\boldsymbol{R}_l = [\boldsymbol{T}_{bl}, -\boldsymbol{E}_{2M\times 1}]$ and $\boldsymbol{n}_l = [n_{l1}, \bar{n}_{l1}, \cdots, n_{lM}, \bar{n}_{lM}]^T$. The vectors

$$\begin{aligned}\boldsymbol{T}_{al} &= [-R_{l1}, \bar{T}_{l1}, \cdots, -R_{lM}, \bar{T}_{lM}]^T \quad \text{and} \\ \boldsymbol{T}_{bl} &= [-T_{l1}, \bar{R}_{l1}, \cdots, -T_{lM}, \bar{R}_{lM}]^T\end{aligned} \tag{8}$$

include the time-stamps at the l^{th} anchor side and the Node B side, respectively. Stacking the $\boldsymbol{T}_l(\boldsymbol{x})$ and $\boldsymbol{R}_l$ from all L anchors, we have

$$\boldsymbol{T}(\boldsymbol{x}) = \boldsymbol{R}\boldsymbol{\theta} - \boldsymbol{n} \tag{9}$$

where $\boldsymbol{T}(\boldsymbol{x}) = [\boldsymbol{T}_1(\boldsymbol{x})^T, \cdots, \boldsymbol{T}_L(\boldsymbol{x})^T]^T$, $\boldsymbol{R} = [\boldsymbol{R}_1^T, \cdots, \boldsymbol{R}_L^T]^T$, and $\boldsymbol{n} = [\boldsymbol{n}_1^T, \cdots, \boldsymbol{n}_L^T]^T$.

Since the error vector is Gaussian distributed, the joint probability density function (PDF) of the observations

$$\boldsymbol{T}_a = \left[\boldsymbol{T}_{a1}^T, \cdots, \boldsymbol{T}_{aL}^T\right]^T \quad \text{and} \quad \boldsymbol{T}_b = \left[\boldsymbol{T}_{b1}^T, \cdots, \boldsymbol{T}_{bL}^T\right]^T \tag{10}$$

conditioned on the unknown vectors $\{\boldsymbol{x}, \boldsymbol{\theta}\}$ is given by

$$\begin{aligned}p_1(\boldsymbol{T}_a, \boldsymbol{T}_b|\boldsymbol{x}, \boldsymbol{\theta}) &= (2\pi|\boldsymbol{C}_n|)^{-LM} \\ &\times \exp\left\{-\frac{1}{2}(\boldsymbol{T}(\boldsymbol{x}) - \boldsymbol{R}\boldsymbol{\theta})^T \boldsymbol{C}_n^{-1}(\boldsymbol{T}(\boldsymbol{x}) - \boldsymbol{R}\boldsymbol{\theta})\right\}\end{aligned} \tag{11}$$

where $\boldsymbol{C}_n$ is the covariance matrix of the error vector $\boldsymbol{n}$. The ML estimate of $\boldsymbol{x}$ and $\boldsymbol{\theta}$ can be obtained by minimizing [22]

$$\Lambda(\boldsymbol{x}, \boldsymbol{\theta}) = (\boldsymbol{T}(\boldsymbol{x}) - \boldsymbol{R}\boldsymbol{\theta})^T \boldsymbol{C}_n^{-1}(\boldsymbol{T}(\boldsymbol{x}) - \boldsymbol{R}\boldsymbol{\theta}). \tag{12}$$

When $\boldsymbol{x}$ is fixed, the minimizing $\boldsymbol{\theta}$ is

$$\hat{\boldsymbol{\theta}} = \left(\boldsymbol{R}^T\boldsymbol{C}_n^{-1}\boldsymbol{R}\right)^{-1}\boldsymbol{R}^T\boldsymbol{C}_n^{-1}\boldsymbol{T}(\boldsymbol{x}). \tag{13}$$

Inserting (13) back to (12), after some straightforward manipulation, the location $\boldsymbol{x}$ can be estimated as

$$\hat{\boldsymbol{x}} = \arg\min_{\boldsymbol{x}}\left\{\|\boldsymbol{P}_1\boldsymbol{T}(\boldsymbol{x})\|^2_{\boldsymbol{C}_n^{-1}}\right\} \tag{14}$$

where $\boldsymbol{P}_1 = \boldsymbol{I} - \boldsymbol{R}(\boldsymbol{R}^T\boldsymbol{C}_n^{-1}\boldsymbol{R})^{-1}\boldsymbol{R}^T\boldsymbol{C}_n^{-1}$, and $\|\boldsymbol{z}\|_{\boldsymbol{W}} = \boldsymbol{z}^T\boldsymbol{W}\boldsymbol{z}$ is the weighted Euclidean norm.

The final estimate of $\boldsymbol{\theta}$ is obtained by inserting the result of (14) back to (13). The two dimensional optimization problem in (14) can be solved by alternating projection as has been reported in [23].

B. Efficient Least Squares Estimator

The above ML method involves solving a two-dimensional nonlinear optimization problem. Although the alternating projection is much more efficient than exhaustive search, it is still computationally expensive and poses a serious problem for the energy constrained sensors. In this subsection, we propose a computationally efficient two-step LS approach, in which closed-form solution exists, to estimate the timing and location parameters of the sensor.

1) Linearization Step: Move the term t_l in (5) and (6) to one side and other terms to the other side, square the two equations and re-arrange them, we have

$$\begin{aligned}&2\left[\frac{1}{c^2}\boldsymbol{x}^T\boldsymbol{a}_l^o - T_{lm}R_{lm}\theta_1 + R_{lm}\theta_2 + \frac{1}{2}T_{lm}^2\theta_1^2 - T_{lm}\theta_1\theta_2\right. \\ &\quad \left.+\frac{1}{2}\left(\theta_2^2 - \frac{1}{c^2}\|\boldsymbol{x}\|^2\right)\right] \\ &\quad = \frac{1}{c^2}\|\boldsymbol{a}_l^o\|^2 - R_{lm}^2 + e_{lm},\end{aligned} \tag{15}$$

$$\begin{aligned}&2\left[\frac{1}{c^2}\boldsymbol{x}^T\boldsymbol{a}_l^o - \bar{T}_{lm}\bar{R}_{lm}\theta_1 + \bar{T}_{lm}\theta_2 + \frac{1}{2}\bar{R}_{lm}^2\theta_1^2 - \bar{R}_{lm}\theta_1\theta_2\right. \\ &\quad \left.+\frac{1}{2}\left(\theta_2^2 - \frac{1}{c^2}\|\boldsymbol{x}\|^2\right)\right] \\ &\quad = \frac{1}{c^2}\|\boldsymbol{a}_l^o\|^2 - \bar{T}_{lm}^2 + \bar{e}_{lm}\end{aligned} \tag{16}$$

where

$$e_{lm} = 2(-T_{lm}\theta_1 + \theta_2 + R_{lm})n_{lm} - n_{lm}^2, \tag{17}$$

$$\bar{e}_{lm} = 2(\bar{R}_{lm}\theta_1 - \theta_2 - \bar{T}_{lm})\bar{n}_{lm} - \bar{n}_{lm}^2 \tag{18}$$

include all the terms involving n_{lm} and $\bar{n}_{lm}$.

By introducing three additional variables $\xi_5 = (1/2)\theta_1^2$, $\xi_6 = (1/2)(\theta_2^2 - \|\boldsymbol{x}\|^2/c^2)$, $\xi_7 = \theta_1\theta_2$ and defining a new vector $\boldsymbol{\xi} = [\boldsymbol{x}^T, \boldsymbol{\theta}^T, \xi_5, \xi_6, \xi_7]^T$, (15) and (16) with $m = 1, 2, \cdots, M$ can be put into a matrix form as

$$\boldsymbol{A}_l\boldsymbol{\xi} = \boldsymbol{b}_l + \boldsymbol{e}_l \tag{19}$$

where

$$\boldsymbol{A}_l = 2\begin{bmatrix}\boldsymbol{a}_l^{oT}/c^2 & -T_{l1}R_{l1} & R_{l1} & T_{l1}^2 & 1 & -T_{l1} \\ \boldsymbol{a}_l^{oT}/c^2 & -\bar{T}_{l1}\bar{R}_{l1} & \bar{T}_{l1} & \bar{R}_{l1}^2 & 1 & -\bar{R}_{l1} \\ & & & \vdots & & \\ \boldsymbol{a}_l^{oT}/c^2 & -T_{lM}R_{lM} & R_{lM} & T_{lM}^2 & 1 & -T_{lM} \\ \boldsymbol{a}_l^{oT}/c^2 & -\bar{T}_{lM}\bar{R}_{lM} & \bar{T}_{lM} & \bar{R}_{lM}^2 & 1 & -\bar{R}_{lM}\end{bmatrix},$$

$$\boldsymbol{b}_l = \begin{bmatrix}\|\boldsymbol{a}_l^o\|^2/c^2 - R_{l1}^2 \\ \|\boldsymbol{a}_l^o\|^2/c^2 - \bar{T}_{l1}^2 \\ \vdots \\ \|\boldsymbol{a}_l^o\|^2/c^2 - R_{lM}^2 \\ \|\boldsymbol{a}_l^o\|^2/c^2 - \bar{T}_{lM}^2\end{bmatrix}, \tag{20}$$

and $\boldsymbol{e}_l = [e_{l1}, \bar{e}_{l1}, \cdots, e_{lM}, \bar{e}_{lM}]^T$. By stacking all the equations for $l = 1, 2, \cdots, L$ together, we have

$$\boldsymbol{A}\boldsymbol{\xi} = \boldsymbol{b} + \boldsymbol{e} \tag{21}$$

where $\boldsymbol{A} = [\boldsymbol{A}_1^T, \cdots, \boldsymbol{A}_L^T]^T$, $\boldsymbol{b} = [\boldsymbol{b}_1^T, \cdots, \boldsymbol{b}_L^T]^T$, and $\boldsymbol{e} = [\boldsymbol{e}_1^T, \cdots, \boldsymbol{e}_L^T]^T$.

Solving (21) in LS sense, we can obtain an estimate of $\boldsymbol{\xi}$ as

$$\hat{\boldsymbol{\xi}}_{\mathrm{LS}} = (\boldsymbol{A}^T\boldsymbol{A})^{-1}\boldsymbol{A}^T\boldsymbol{b}. \tag{22}$$

However, note that (22) only provides a rough estimate of the unknown vectors $\boldsymbol{x}$ and $\boldsymbol{\theta}$, because of two reasons. First, the estimator (22) assumes all the components in the measurement error vector $\boldsymbol{e}$ have the same variances, while it is obviously not the case as can be seen from (17). Second, there is no constraints applied between the elements of $\boldsymbol{\xi}$ in (22), and thus the estimate may be inconsistent. Next, we propose a second step to improve the estimate of (22) based on the above two observations.

2) Refinement Step: Notice that the second-order terms in the noise vector $\boldsymbol{e}$ can be ignored because n_{lm}^2 and $\bar{n}_{lm}^2$ are usually very small. Therefore, from (17), $\boldsymbol{e}$ can be approximated by $\boldsymbol{e} \approx 2\boldsymbol{T}_e \odot \boldsymbol{n}$, where $\boldsymbol{T}_e = \theta_1\boldsymbol{T}_b - \theta_2\boldsymbol{E}_{2M\times 1} - \boldsymbol{T}_a$. The covariance matrix of the noise vector $\boldsymbol{e}$ can then be derived as $\boldsymbol{C}_e \approx 4(\boldsymbol{T}_e\boldsymbol{T}_e^T) \odot \boldsymbol{C}_n$. Notice that $\boldsymbol{C}_e$ depends on θ_1 and θ_2, which are also parameters of interest. Fortunately, we can use the rough estimate in (22) of step 1. The weighted least square (WLS) solution of (21) is then given by

$$\hat{\boldsymbol{\xi}}_{\mathrm{WLS}} = \left(\boldsymbol{A}^T\hat{\boldsymbol{C}}_e^{-1}\boldsymbol{A}\right)^{-1}\boldsymbol{A}^T\hat{\boldsymbol{C}}_e^{-1}\boldsymbol{b} \tag{23}$$

where $\hat{\boldsymbol{C}}_e$ is $\boldsymbol{C}_e$ with θ_1 and θ_2 replaced by $\hat{\theta}_1$ and $\hat{\theta}_2$ from (22).

Next, the relationships between elements of $\boldsymbol{\xi}$ are exploited, which can be put into the following matrix form:

$$\hat{\boldsymbol{G}}_1\boldsymbol{\omega} = \hat{\boldsymbol{\xi}}_{\mathrm{WLS}} + \boldsymbol{n}_{\mathrm{WLS}} \tag{24}$$

where

$$\boldsymbol{\omega} = \begin{bmatrix}\boldsymbol{x}\\ \boldsymbol{\theta}\end{bmatrix},\ \hat{\boldsymbol{G}}_1 = \begin{bmatrix}\boldsymbol{I}_4\\ \tilde{\boldsymbol{G}}_1\end{bmatrix}$$
$$\tilde{\boldsymbol{G}}_1 = \frac{1}{2}\begin{bmatrix}0 & 0 & \hat{\theta}_1 & 0\\ -\frac{\hat{x}}{c^2} & -\frac{\hat{y}}{c^2} & 0 & \hat{\theta}_2\\ 0 & 0 & \hat{\theta}_2 & \hat{\theta}_1\end{bmatrix} \tag{25}$$

and $\boldsymbol{n}_{\mathrm{WLS}}$ is the estimation error in $\hat{\boldsymbol{\xi}}_{\mathrm{WLS}}$. Together with the fact that the estimation covariance of $\hat{\boldsymbol{\xi}}_{\mathrm{WLS}}$ is $\boldsymbol{C}_{\mathrm{WLS}} = (\boldsymbol{A}^T\hat{\boldsymbol{C}}_e^{-1}\boldsymbol{A})^{-1}$ [22], the WLS solution of (24) is

$$\begin{aligned}\hat{\boldsymbol{\omega}}_{\mathrm{CWLS}} &= \left(\hat{\boldsymbol{G}}_1^T\boldsymbol{C}_{\mathrm{WLS}}^{-1}\hat{\boldsymbol{G}}_1\right)^{-1}\hat{\boldsymbol{G}}_1^T\boldsymbol{C}_{\mathrm{WLS}}^{-1}\hat{\boldsymbol{\xi}}_{\mathrm{WLS}}\\ &= \left(\hat{\boldsymbol{G}}_1^T\boldsymbol{A}^T\hat{\boldsymbol{C}}_e^{-1}\boldsymbol{A}\hat{\boldsymbol{G}}_1\right)^{-1}\hat{\boldsymbol{G}}_1^T\boldsymbol{A}^T\hat{\boldsymbol{C}}_e^{-1}\boldsymbol{b}.\end{aligned} \tag{26}$$

Notice that the proposed CWLS estimator (26) is in closed form and does not need a searching step as in the ML estimator (14). The final estimates of θ_s and θ_0 are obtained from the estimates $\hat{\theta}_1$ and $\hat{\theta}_2$ in (26) by $\hat{\theta}_s = 1/\hat{\theta}_1$ and $\hat{\theta}_0 = \hat{\theta}_2/\hat{\theta}_1$.

IV. Joint Synchronization and Localization With Anchor Uncertainties

In WSNs, when a large number of sensors need to be synchronized or localized, it is a common procedure that synchronization and localization are performed level by level [7]. The sensor nodes closest to anchors are synchronized and localized first. Then, they become the new anchors and other nearby sensors perform synchronization and localization with the new anchors. This process is repeated until all the nodes are synchronized and localized.

Because of this level-by-level procedure, the new anchors do not have perfect timing and location information of their own. We refer the inaccuracies of the anchor timing and location as anchor uncertainties. If we use these new anchors to synchronize and localize other nodes in the sensor network, it is important to take the anchor uncertainties into account.

A. Model of Uncertainties and ML Estimator

When there are anchor uncertainties, we can only have the observed (but not true) values of the location, time skew and time offset of anchors

$$\boldsymbol{a}_l = \boldsymbol{a}_l^o - \Delta\boldsymbol{a}_l,\ \theta_{sl} = \theta_{sl}^o - \Delta\theta_{sl},\ \theta_{0l} = \theta_{0l}^o - \Delta\theta_{0l} \tag{27}$$

where $\Delta\boldsymbol{a}_l = [\Delta a_{xl}, \Delta a_{yl}]^T$, $\Delta\theta_{sl}$, $\Delta\theta_{0l}$ are the uncertainties in the l^{th} anchor's location, time skew and time offset, respectively. It is assumed that $\Delta\boldsymbol{a}_l$, $\Delta\theta_{sl}$, and $\Delta\theta_{0l}$ are Gaussian distributed. Notice that the errors in the anchor timings and locations are unnecessarily independent, depending on how the timings and locations of the anchors are estimated. For example, if the timings and locations of anchors are estimated by the joint estimator in Section III, the anchor timing and location errors are actually correlated. On the other hand, if the timings and locations of anchors are estimated separately using different observations, the estimation errors can be uncorrelated. In order to keep the discussion more general, all the measured anchor timings and locations are grouped into a vector $\boldsymbol{k} = [a_{x1}, a_{y1}, \theta_{s1}, \theta_{01}, \cdots, a_{xL}, a_{yL}, \theta_{sL}, \theta_{0L}]^T$ with the true (but unknown) value denoted as $\boldsymbol{k}^o$, and whose covariance matrix is denoted by $\boldsymbol{C}_k$. It is assumed that the covariance matrix of the anchor uncertainties is known.

Dividing both sides of (1) and (2) by θ_s, the equations for the l^{th} anchor can be grouped into $\boldsymbol{T}_{bl}/\theta_s = \boldsymbol{T}_{al}/\theta_{sl}^o + t_l \otimes \boldsymbol{1}_{2M\times 1} + (\theta_0/\theta_s - \theta_{0l}^o/\theta_{sl}^o)\boldsymbol{E}_{2M\times 1} + \boldsymbol{n}_l$, where $\boldsymbol{T}_{al}$ and $\boldsymbol{T}_{bl}$ were defined in (8), and $\boldsymbol{n}_l$ was defined when introducing (7). Further, stacking the equations for all L anchors, we have $\boldsymbol{T}_b/\theta_s = \boldsymbol{\mu} + \boldsymbol{n}$, where

$$\begin{aligned}\boldsymbol{\mu} = \boldsymbol{T}_a \odot \left(\begin{bmatrix}1/\theta_{s1}^o\\ \vdots\\ 1/\theta_{sL}^o\end{bmatrix} \otimes \boldsymbol{1}_{2M\times 1}\right) + \begin{bmatrix}t_1\\ \vdots\\ t_L\end{bmatrix} \otimes \boldsymbol{1}_{2M\times 1}\\ + \frac{\theta_0}{\theta_s}\boldsymbol{E}_{2LM\times 1} - \begin{bmatrix}\theta_{01}^o/\theta_{s1}^o\\ \vdots\\ \theta_{0L}^o/\theta_{sL}^o\end{bmatrix} \otimes \boldsymbol{E}_{2M\times 1}.\end{aligned} \tag{28}$$

Because all the measurement errors are Gaussian and the errors in observed time-stamps are independent of errors in anchor timing and location parameters, the logarithm of the joint PDF of the observed time-stamps, anchor timings and locations is then given by

$$\begin{aligned}&\ln p_2\left(\boldsymbol{T}_a, \boldsymbol{T}_b, \{\boldsymbol{a}_l, \theta_{sl}, \theta_{0l}\}_{l=1}^L | \boldsymbol{x}, \boldsymbol{\theta}, \{\boldsymbol{a}_l^o, \theta_{sl}^o, \theta_{0l}^o\}_{l=1}^L\right)\\ &\quad = d - \frac{1}{2}(\boldsymbol{T}_b/\theta_s - \boldsymbol{\mu})^T\boldsymbol{C}_n^{-1}(\boldsymbol{T}_b/\theta_s - \boldsymbol{\mu})\\ &\qquad - \frac{1}{2}(\boldsymbol{k} - \boldsymbol{k}^o)^T\boldsymbol{C}_k^{-1}(\boldsymbol{k} - \boldsymbol{k}^o)\end{aligned} \tag{29}$$

where d is a constant, and $\boldsymbol{T}_a$ and $\boldsymbol{T}_b$ were introduced in (10).

As can be seen from (29), the joint PDF includes the terms of anchor timing and location uncertainties. Therefore, the ML

joint synchronization and localization involves the maximization with respect to timings and locations of both the unknown node and anchors. Depending on the number of anchors, the problem can be a very high dimensional maximization problem. Even if it is solvable, the ML estimation requires a lot of computations. In the next subsection, we propose a low complexity method instead.

B. Proposed Low-Complexity Least Squares Estimator

Taking anchor uncertainties into account, the exchanged time-stamps in (1) and (2) become

$$\begin{aligned} -T_{lm} = &-\frac{\theta_s}{\theta_{sl}+\Delta\theta_{sl}}R_{lm}+\theta_s(t_l+n_{lm})-\theta_0 \\ &+\frac{\theta_s}{\theta_{sl}+\Delta\theta_{sl}}(\theta_{0l}+\Delta\theta_{0l}) \end{aligned} \tag{30}$$

$$\begin{aligned} \bar{R}_{lm} = &\frac{\theta_s}{\theta_{sl}+\Delta\theta_{sl}}\bar{T}_{lm}+\theta_s(t_l+\bar{n}_{lm})+\theta_0 \\ &-\frac{\theta_s}{\theta_{sl}+\Delta\theta_{sl}}(\theta_{0l}+\Delta\theta_{0l}). \end{aligned} \tag{31}$$

Dividing both sides of (30) and (31) by θ_s, and using the first-order Taylor series approximation $1/(\theta_{sl}+\Delta\theta_{sl}) \approx 1/\theta_{sl} - \Delta\theta_{sl}/\theta_{sl}^2$, we have

$$\begin{aligned} -T_{lm}\theta_1 \approx &-\frac{R_{lm}-\theta_{0l}}{\theta_{sl}}-\theta_2+t_l+n_{lm} \\ &+\frac{R_{lm}-\theta_{0l}}{\theta_{sl}^2}\Delta\theta_{sl}+\frac{1}{\theta_{sl}}\Delta\theta_{0l} \end{aligned} \tag{32}$$

$$\begin{aligned} \bar{R}_{lm}\theta_1 \approx &\frac{\bar{T}_{lm}-\theta_{0l}}{\theta_{sl}}+\theta_2+t_l+\bar{n}_{lm} \\ &-\frac{\bar{T}_{lm}-\theta_{0l}}{\theta_{sl}^2}\Delta\theta_{sl}-\frac{1}{\theta_{sl}}\Delta\theta_{0l} \end{aligned} \tag{33}$$

where we have neglected the second-order terms of the anchor timing errors.

Representing t_l as $t_l = \|\boldsymbol{x}-(\boldsymbol{a}_l+\Delta\boldsymbol{a}_l)\|/c$ and using the same linearization procedure as in Section III-B, (32) and (33) can be formulated into a linear equation as

$$(\underline{\boldsymbol{A}}+\Delta\boldsymbol{A})\boldsymbol{\xi} = \underline{\boldsymbol{b}}+\boldsymbol{v}, \tag{34}$$

where $\underline{\boldsymbol{A}} \triangleq [\underline{\boldsymbol{A}}_1, \underline{\boldsymbol{A}}_2, \cdots, \underline{\boldsymbol{A}}_L]^T$ and $\underline{\boldsymbol{b}} \triangleq [\underline{\boldsymbol{b}}_1, \underline{\boldsymbol{b}}_2, \cdots, \underline{\boldsymbol{b}}_L]^T$ with (35) and (36), shown at the bottom of the page. The perturbation terms in (34) are given by

$$\Delta\boldsymbol{A} = \Bigg[\underbrace{\frac{2}{c^2}[\Delta\boldsymbol{a}_1,\cdots,\Delta\boldsymbol{a}_L]^T\otimes\boldsymbol{1}_{2M\times 1}}_{\triangleq\delta\boldsymbol{A}}, \boldsymbol{0}_{2LM\times 5}\Bigg], \tag{37}$$

$$\boldsymbol{v} = \underbrace{\frac{2}{c^2}\left[\boldsymbol{a}_1^T\Delta\boldsymbol{a}_1,\cdots,\boldsymbol{a}_L^T\Delta\boldsymbol{a}_L\right]^T\otimes\boldsymbol{1}_{2M\times 1}}_{\triangleq\Delta\boldsymbol{b}}+\boldsymbol{e}', \tag{38}$$

and the error vector $\boldsymbol{e}' \triangleq [e'_{11}, \bar{e}'_{11}, \cdots, e'_{LM}, \bar{e}'_{LM}]^T$ with

$$\begin{aligned} e'_{lm} = &2\left(-T_{lm}\theta_1+\theta_2+(R_{lm}-\theta_{0l})/\theta_{sl}\right) \\ &\times\left(n_{lm}+(R_{l1}-\theta_{0l})\Delta\theta_{sl}/\theta_{sl}^2+\Delta\theta_{0l}/\theta_{sl}\right)+\mathcal{O} \end{aligned} \tag{39}$$

$$\begin{aligned} \bar{e}'_{lm} = &2\left(\bar{R}_{lm}\theta_1-\theta_2-(\bar{T}_{lm}-\theta_{0l})/\theta_{sl}\right) \\ &\times\left(\bar{n}_{lm}-(\bar{T}_{lm}-\theta_{0l})\Delta\theta_{sl}/\theta_{sl}^2-\Delta\theta_{0l}/\theta_{sl}\right)+\mathcal{O}, \end{aligned} \tag{40}$$

where $\mathcal{O}$ represents the second-order terms of the anchor uncertainties and TOA detection errors. Note that when there is no uncertainty in the anchors and the true anchor timing parameters are $\theta_{sl}^o = 1$ and $\theta_{0l}^o = 0$, (34) reduces to (21).

Because $\Delta\boldsymbol{A}$ and $\Delta\boldsymbol{b}$ in (37) and (38) are unknown, the true system model (34) should be replaced by the following observation model

$$\underline{\boldsymbol{A}}\boldsymbol{\xi} = \underline{\boldsymbol{b}}+\boldsymbol{e}'. \tag{41}$$

Equation (41) can be interpreted as a linear system with model error in the model coefficient matrix $\underline{\boldsymbol{A}}$. The generalized total least square (GTLS) technique can be employed to provide consistent estimate of $\boldsymbol{\xi}$ [25]. The GTLS method aims to find a solution that minimizes the total weighted error in the expanded matrix $[\underline{\boldsymbol{A}}\ \underline{\boldsymbol{b}}]$. For notational simplicity, the coefficient matrix $\underline{\boldsymbol{A}}$ is first permutated by a permutation matrix $\boldsymbol{P}$ such that only the right most columns of $[\underline{\boldsymbol{A}}\ \underline{\boldsymbol{b}}]$ are subject to errors:

$$\underbrace{\underline{\boldsymbol{A}}\boldsymbol{P}}_{\triangleq\boldsymbol{H}}\underbrace{\boldsymbol{P}^{-1}\boldsymbol{\xi}}_{\triangleq\underline{\boldsymbol{\xi}}} \approx \underbrace{\underline{\boldsymbol{b}}+\boldsymbol{e}'}_{\triangleq\boldsymbol{\epsilon}} \tag{42}$$

where $\boldsymbol{H}$ (permutated version of $\boldsymbol{A}$) can be partitioned into $\boldsymbol{H} = [\boldsymbol{H}_1\ \boldsymbol{H}_2]$, with $\boldsymbol{H}_2$ (the first two columns of $\underline{\boldsymbol{A}}$) subject to errors,

$$\underline{\boldsymbol{A}}_l = 2\begin{bmatrix} \boldsymbol{a}_l^T/c^2 & -T_{l1}(R_{l1}-\theta_{0l})/\theta_{sl} & (R_{l1}-\theta_{0l})/\theta_{sl} & T_{l1}^2 & 1 & -T_{l1} \\ \boldsymbol{a}_l^T/c^2 & -\bar{R}_{l1}(\bar{T}_{l1}-\theta_{0l})/\theta_{sl} & (\bar{T}_{l1}-\theta_{0l})/\theta_{sl} & \bar{R}_{l1}^2 & 1 & -\bar{R}_{l1} \\ & & & \vdots & & \\ \boldsymbol{a}_l^T/c^2 & -T_{lM}(R_{LM}-\theta_{0l})/\theta_{sl} & (R_{LM}-\theta_{0l})/\theta_{sl} & T_{lM}^2 & 1 & -T_{lM} \\ \boldsymbol{a}_l^T/c^2 & -\bar{R}_{lM}(\bar{T}_{LM}-\theta_{0l})/\theta_{sl} & (\bar{T}_{LM}-\theta_{0l})/\theta_{sl} & \bar{R}_{lM}^2 & 1 & -\bar{R}_{lM} \end{bmatrix}, \tag{35}$$

$$\underline{\boldsymbol{b}}_l = \begin{bmatrix} \|\boldsymbol{a}_l\|^2/c^2-(R_{l1}-\theta_{0l})^2/\theta_{sl}^2 \\ \|\boldsymbol{a}_l\|^2/c^2-(\bar{T}_{l1}-\theta_{0l})^2/\theta_{sl}^2 \\ \vdots \\ \|\boldsymbol{a}_l\|^2/c^2-(R_{LM}-\theta_{0l})^2/\theta_{sl}^2 \\ \|\boldsymbol{a}_l\|^2/c^2-(\bar{T}_{LM}-\theta_{0l})^2/\theta_{sl}^2 \end{bmatrix}. \tag{36}$$

and $\boldsymbol{H}_1$ (the rest of the columns of $\underline{\boldsymbol{A}}$) free of error. For GTLS method, the minimization of weighted error in both $\underline{\boldsymbol{A}}$ and $\underline{\boldsymbol{b}}$ is represented by [24]

$$\min_{[\hat{\boldsymbol{H}}_2\ \hat{\boldsymbol{\epsilon}}]} \left\| \left([\boldsymbol{H}_2\ \boldsymbol{\epsilon}] - [\hat{\boldsymbol{H}}_2\ \hat{\boldsymbol{\epsilon}}] \right) \boldsymbol{C}_U^{-1/2} \right\|_F \quad \text{subject to} \quad \hat{\boldsymbol{\epsilon}} \in \mathcal{R}\left([\boldsymbol{H}_1\ \hat{\boldsymbol{H}}_2] \right) \tag{43}$$

where $\boldsymbol{C}_U$ is the covariance matrix of $\boldsymbol{U}^T$ (with $\boldsymbol{U} \triangleq [\delta\boldsymbol{A}, \boldsymbol{v}]$)

$$\boldsymbol{C}_U = \mathbb{E}\{\boldsymbol{U}^T\boldsymbol{U}\} \triangleq \begin{bmatrix} \boldsymbol{C}_A & \boldsymbol{c}_{Av} \\ \boldsymbol{c}_{Av}^T & c_v \end{bmatrix}, \tag{44}$$

symbol $\mathcal{R}(\cdot)$ represents the range space of a matrix, and $\boldsymbol{C}^{1/2}$ is the Cholesky decomposition of $\boldsymbol{C}$. In (44), the expressions for the 2×2 matrix $\boldsymbol{C}_A$, 2×1 vector $\boldsymbol{c}_{Av}$, and the scalar c_v are derived in the Appendix and are given by (80)–(82). Once a $[\hat{\boldsymbol{H}}_2\ \hat{\boldsymbol{\epsilon}}]$ that minimizes the objective function in (43) is found, then any $\underline{\boldsymbol{\xi}}$ satisfying $[\boldsymbol{H}_1\ \hat{\boldsymbol{H}}_2]\underline{\boldsymbol{\xi}} = \hat{\boldsymbol{\epsilon}}$ is a GTLS solution to the problem in (42).

From [25], the closed-form solution of the GTLS problem (43) is

$$\hat{\underline{\boldsymbol{\xi}}}_{\mathrm{GTLS}} = (\boldsymbol{H}^T\boldsymbol{H} - \gamma^2\tilde{\boldsymbol{C}}_A)^{-1}(\boldsymbol{H}^T\boldsymbol{\epsilon} - \gamma^2\tilde{\boldsymbol{c}}_{Av}), \tag{45}$$

where $\tilde{\boldsymbol{C}}_A = \mathrm{diag}[\boldsymbol{0}_{5\times5},\ \boldsymbol{C}_A]$, $\tilde{\boldsymbol{c}}_{Av} = [\boldsymbol{0}_{1\times5},\ \boldsymbol{c}_{Av}^T]^T$ and γ is the smallest generalized singular value of the matrix pair $([\boldsymbol{H}\ \boldsymbol{\epsilon}], \mathrm{diag}[\boldsymbol{0}_{5\times5},\ \boldsymbol{C}_U^{1/2}])$.

After the GTLS solution is obtained, the relationship between elements of $\hat{\underline{\boldsymbol{\xi}}}_{\mathrm{GTLS}}$ can be written similarly as that in (24)

$$\hat{\boldsymbol{G}}_2\boldsymbol{\omega} = \hat{\underline{\boldsymbol{\xi}}}_{\mathrm{GTLS}} + \boldsymbol{n}_{\mathrm{GTLS}} \tag{46}$$

where $\boldsymbol{n}_{\mathrm{GTLS}}$ is the estimation error in $\hat{\underline{\boldsymbol{\xi}}}_{\mathrm{GTLS}}$, and $\hat{\boldsymbol{G}}_2 = [\boldsymbol{I}_4\ \tilde{\boldsymbol{G}}_2^T]^T\boldsymbol{P}$ with $\tilde{\boldsymbol{G}}_2$ obtained by replacing the estimates of $\hat{x}$, $\hat{y}$, $\hat{\theta}_1$ and $\hat{\theta}_2$ in $\tilde{\boldsymbol{G}}_1$ of (25) with their corresponding estimates in $\hat{\underline{\boldsymbol{\xi}}}_{\mathrm{GTLS}}$ of (45).

To carry out the refinement in (46), the estimation covariance of $\hat{\underline{\boldsymbol{\xi}}}_{\mathrm{GTLS}}$, defined as $\boldsymbol{C}_{\mathrm{GTLS}} = \mathbb{E}\{(\hat{\underline{\boldsymbol{\xi}}}_{\mathrm{GTLS}} - \underline{\boldsymbol{\xi}})(\hat{\underline{\boldsymbol{\xi}}}_{\mathrm{GTLS}} - \underline{\boldsymbol{\xi}})^T\}$, is needed. With the expression of $\hat{\underline{\boldsymbol{\xi}}}_{\mathrm{GTLS}}$ in (45), we have

$$\begin{aligned} \hat{\underline{\boldsymbol{\xi}}}_{\mathrm{GTLS}} - \underline{\boldsymbol{\xi}} &= \bar{\boldsymbol{\Gamma}}(\boldsymbol{H}^T\boldsymbol{\epsilon} - \gamma^2\tilde{\boldsymbol{c}}_{Av}) - \bar{\boldsymbol{\Gamma}}\boldsymbol{\Gamma}^{-1}\underline{\boldsymbol{\xi}} \\ &= \boldsymbol{\Gamma}\left[(\boldsymbol{H}^T\boldsymbol{\epsilon} - \gamma^2\tilde{\boldsymbol{c}}_{Av}) - (\boldsymbol{H}^T\boldsymbol{H} - \gamma^2\tilde{\boldsymbol{C}}_A)\underline{\boldsymbol{\xi}} \right] \end{aligned} \tag{47}$$

where $\bar{\boldsymbol{\Gamma}} \triangleq (\boldsymbol{H}^T\boldsymbol{H} - \gamma^2\tilde{\boldsymbol{C}}_A)^{-1}$. The correction effect of $\gamma^2\tilde{\boldsymbol{c}}_{Av}$ and $\gamma^2\tilde{\boldsymbol{C}}_A$ leads to [24]

$$\begin{aligned} \boldsymbol{H}^T\boldsymbol{\epsilon} - \gamma^2\tilde{\boldsymbol{c}}_{Av} &\approx \boldsymbol{H}^{oT}\underline{\boldsymbol{b}}^o \\ \boldsymbol{H}^T\boldsymbol{H} - \gamma^2\tilde{\boldsymbol{C}}_A &\approx \boldsymbol{H}^{oT}\boldsymbol{H}^o \end{aligned} \tag{48}$$

where $\boldsymbol{H}^o = \underline{\boldsymbol{A}}^o\boldsymbol{P}$ with $\underline{\boldsymbol{A}}^o$ and $\underline{\boldsymbol{b}}^o$ are $\underline{\boldsymbol{A}}$ and $\underline{\boldsymbol{b}}$ with accurate anchor locations and timing, respectively. Substituting (48) back into (47) we have

$$\hat{\underline{\boldsymbol{\xi}}}_{\mathrm{GTLS}} - \underline{\boldsymbol{\xi}} \approx \boldsymbol{\Gamma}\boldsymbol{H}^{oT}(\boldsymbol{b}^o - \boldsymbol{H}^o\underline{\boldsymbol{\xi}}) = \boldsymbol{\Gamma}\boldsymbol{H}^{oT}\boldsymbol{v} \tag{49}$$

where we have used the fact that $\boldsymbol{b}^o - \boldsymbol{H}^o\underline{\boldsymbol{\xi}} = \boldsymbol{v}$. Using (49), the covariance matrix of $\hat{\underline{\boldsymbol{\xi}}}_{\mathrm{GTLS}}$ is calculated as

$$\boldsymbol{C}_{\mathrm{GTLS}} = \mathbb{E}\left\{ (\hat{\underline{\boldsymbol{\xi}}}_{\mathrm{GTLS}} - \underline{\boldsymbol{\xi}})(\hat{\underline{\boldsymbol{\xi}}}_{\mathrm{GTLS}} - \underline{\boldsymbol{\xi}})^T \right\} \approx \boldsymbol{\Gamma}\boldsymbol{H}^{oT}\boldsymbol{C}_v\boldsymbol{H}^o\boldsymbol{\Gamma}^T \tag{50}$$

where $\boldsymbol{C}_v = \mathbb{E}\{\boldsymbol{v}\boldsymbol{v}^T\}$ is the covariance matrix of $\boldsymbol{v}$ and is given by (74) in the Appendix. The constrained problem in (46) is therefore solved as

$$\hat{\boldsymbol{\omega}}_{\mathrm{CGTLS}} = \left(\hat{\boldsymbol{G}}_2^T\boldsymbol{C}_{\mathrm{GTLS}}^{-1}\hat{\boldsymbol{G}}_2 \right)^{-1} \hat{\boldsymbol{G}}_2^T\boldsymbol{C}_{\mathrm{GTLS}}^{-1}\hat{\underline{\boldsymbol{\xi}}}_{\mathrm{GTLS}}. \tag{51}$$

Remark 1: In implementation, the closed-form solution in (45) is typically not used to solve the GTLS problem because it is generally numerically unstable. A numerically stable and efficient procedure for obtaining the GTLS solution, which does not involve any matrix inversion, is presented in [25].

Remark 2: Some approximations are needed in carrying out the proposed algorithm. The calculation of $\boldsymbol{C}_U$ requires the true values of $\theta_1 = 1/\theta_s$ and $\theta_2 = \theta_0/\theta_s$. Furthermore, the computation of covariance $\boldsymbol{C}_{\mathrm{GTLS}}$ in (50) requires $\boldsymbol{H}^o$, which in turn requires the accurate locations of anchors. In practice, θ_s and θ_0 are approximated by their nominal values 1 and 0, respectively, and $\boldsymbol{C}_{\mathrm{GTLS}}$ is approximated by $\hat{\boldsymbol{C}}_{\mathrm{GTLS}} \approx \boldsymbol{\Gamma}\boldsymbol{H}^T\boldsymbol{C}_v\boldsymbol{H}\boldsymbol{\Gamma}^T$, where the accurate anchor locations in $\boldsymbol{H}^o$ are approximated by their observations in $\boldsymbol{H}$. The performance degradation due to the approximation in weighting matrices is insignificant as has been demonstrated in [26].

Remark 3: By ignoring the anchor uncertainties in (41), we can also apply the LS based algorithm (26) in Section III-B and obtain the following estimate:

$$\underline{\boldsymbol{w}}_{\mathrm{CWLS}} = \left(\underline{\boldsymbol{G}}_1^T\boldsymbol{H}^T\boldsymbol{C}_v^{-1}\boldsymbol{H}\underline{\boldsymbol{G}}_1 \right)^{-1} \underline{\boldsymbol{G}}_1^T\boldsymbol{H}^T\boldsymbol{C}_v^{-1}\underline{\boldsymbol{b}} \tag{52}$$

where $\underline{\boldsymbol{G}}_1$ is obtained by replacing the estimates of $\hat{x}$, $\hat{y}$, $\hat{\theta}_1$ and $\hat{\theta}_2$ in $\tilde{\boldsymbol{G}}_1$ of (25) with their corresponding estimates in $\hat{\underline{\boldsymbol{\xi}}}_{\mathrm{LS}} = (\underline{\boldsymbol{A}}^T\underline{\boldsymbol{A}})^{-1}\underline{\boldsymbol{A}}^T\underline{\boldsymbol{b}}$.

Summary: The proposed low-complexity LS estimator under anchor uncertainties is summarized as follows.

1) Formulate the observation model (41).
2) Compute the GTLS solution (45) using the numerical method given in [25].
3) Refine the GTLS solution by (51).

V. Performance Analyses

In order to provide a performance reference for the proposed estimators, the CRLBs of the joint synchronization and localization problem for both cases with accurate and inaccurate anchors are derived. The analytical MSEs of the proposed LS estimators are also derived. To distinguish the two proposed LS algorithms in Sections III and IV, we refer the LS algorithm in (26) as LS-I and that in (51) as LS-II, respectively.

A. CRLB With Accurate Anchors

With $\boldsymbol{\Phi} = [\boldsymbol{x}^T, \theta_s, \theta_0]^T$ and the joint PDF in (11), the CRLB can be derived as [22]

$$\begin{aligned}\mathrm{CRLB}(\boldsymbol{\Phi}) &= -\left[\mathbb{E}\left\{\frac{\partial^2 \ln p_1}{\partial \boldsymbol{\Phi} \partial \boldsymbol{\Phi}^T}\right\}\right]^{-1} \\ &= \left[\left\{\frac{\partial \boldsymbol{\eta}}{\partial \boldsymbol{\Phi}}\right\}^T \boldsymbol{C}_n^{-1} \left\{\frac{\partial \boldsymbol{\eta}}{\partial \boldsymbol{\Phi}}\right\}\right]^{-1} \end{aligned} \tag{53}$$

where $\boldsymbol{\eta} = \boldsymbol{T}(\boldsymbol{x}) - \boldsymbol{R}\boldsymbol{\theta}$, and the second equality above is obtained after taking the expectation. The partial derivative can be computed as

$$\frac{\partial \boldsymbol{\eta}}{\partial \boldsymbol{\Phi}} = [\boldsymbol{B}_1 \; \boldsymbol{B}_2] \triangleq \boldsymbol{B} \tag{54}$$

where

$$\begin{aligned}\boldsymbol{B}_1 &= \frac{1}{c^2}\left[(\boldsymbol{x} - \boldsymbol{a}_1^o)^T/t_1, \cdots, (\boldsymbol{x} - \boldsymbol{a}_L^o)^T/t_L\right]^T \otimes \mathbf{1}_{2M\times 1} \\ \boldsymbol{B}_2 &= \left[\frac{1}{\theta_s^2}(-\boldsymbol{T}_b + \theta_0 \boldsymbol{E}_{2LM\times 1}), \frac{1}{\theta_s}\boldsymbol{E}_{2LM\times 1}\right]. \end{aligned} \tag{55}$$

Therefore, $\mathrm{CRLB}(\boldsymbol{\Phi}) = (\boldsymbol{B}^T \boldsymbol{C}_n^{-1} \boldsymbol{B})^{-1}$. Note that, as special cases, the CRLB of location estimate with perfect timing and the CRLB of timing estimate with perfect location are given by $\mathrm{CRLB}(\boldsymbol{x}) = (\boldsymbol{B}_1^T \boldsymbol{C}_n^{-1} \boldsymbol{B}_1)^{-1}$ and $\mathrm{CRLB}([\theta_s, \theta_0]^T) = (\boldsymbol{B}_2^T \boldsymbol{C}_n^{-1} \boldsymbol{B}_2)^{-1}$, respectively.

B. CRLB With Anchor Uncertainties

With the joint PDF in (29), the CRLB of $\boldsymbol{\Upsilon} = [\boldsymbol{\Phi}^T, \boldsymbol{k}^{oT}]^T$ is derived as [22]

$$\mathrm{CRLB}(\boldsymbol{\Upsilon}) = -\left[\mathbb{E}\left\{\frac{\partial^2 \ln p_2}{\partial \boldsymbol{\Upsilon} \partial \boldsymbol{\Upsilon}^T}\right\}\right]^{-1} = \begin{bmatrix} \boldsymbol{S}_1 & \boldsymbol{S}_2 \\ \boldsymbol{S}_2^T & \boldsymbol{S}_3 \end{bmatrix}^{-1} \tag{56}$$

where

$$\begin{aligned}\boldsymbol{S}_1 &= -\mathbb{E}\left\{\frac{\partial^2 \ln p_2}{\partial \boldsymbol{\Phi} \partial \boldsymbol{\Phi}^T}\right\} = \left\{\frac{\partial \boldsymbol{\zeta}}{\partial \boldsymbol{\Phi}}\right\}^T \boldsymbol{C}_n^{-1} \left\{\frac{\partial \boldsymbol{\zeta}}{\partial \boldsymbol{\Phi}}\right\} \\ \boldsymbol{S}_2 &= -\mathbb{E}\left\{\frac{\partial^2 \ln p_2}{\partial \boldsymbol{\Phi} \partial \boldsymbol{k}^{oT}}\right\} = \left\{\frac{\partial \boldsymbol{\zeta}}{\partial \boldsymbol{\Phi}}\right\}^T \boldsymbol{C}_n^{-1} \left\{\frac{\partial \boldsymbol{\mu}}{\partial \boldsymbol{k}^o}\right\} \\ \boldsymbol{S}_3 &= -\mathbb{E}\left\{\frac{\partial^2 \ln p_2}{\partial \boldsymbol{k}^o \partial \boldsymbol{k}^{oT}}\right\} = \left\{\frac{\partial \boldsymbol{\mu}}{\partial \boldsymbol{k}^o}\right\}^T \boldsymbol{C}_n^{-1} \left\{\frac{\partial \boldsymbol{\mu}}{\partial \boldsymbol{k}^o}\right\} + \boldsymbol{C}_k^{-1} \end{aligned} \tag{57}$$

with $\boldsymbol{\zeta} = \boldsymbol{T}_b/\theta_s - \boldsymbol{\mu}$. The partial derivatives in the above equations are derived as

$$\frac{\partial \boldsymbol{\zeta}}{\partial \boldsymbol{\Phi}} = \boldsymbol{B}, \quad \frac{\partial \boldsymbol{\mu}}{\partial \boldsymbol{k}^o} = \mathrm{diag}[\boldsymbol{D}_1, \cdots, \boldsymbol{D}_L] \tag{58}$$

where

$$\begin{aligned}\boldsymbol{D}_l = \Big[&(\boldsymbol{a}_l^o - \boldsymbol{x})^T \otimes \mathbf{1}_{2M\times 1}/(c^2 t_l), \\ &(-\boldsymbol{T}_{al} + \theta_{0l}\boldsymbol{E}_{2M\times 1})/\theta_{sl}^{o2}, -\boldsymbol{E}_{2M\times 1}/\theta_{sl}^o\Big] \end{aligned} \tag{59}$$

with $\boldsymbol{T}_{al}$ defined in (8).

Using the matrix inversion lemma, the CRLB for $\boldsymbol{\Phi}$ is given by

$$\mathrm{CRLB}(\boldsymbol{\Phi}) = \boldsymbol{S}_1^{-1} + \boldsymbol{S}_1^{-1}\boldsymbol{S}_2\left(\boldsymbol{S}_3 - \boldsymbol{S}_2^T \boldsymbol{S}_{11}^{-1} \boldsymbol{S}_2\right)^{-1} \boldsymbol{S}_2^T \boldsymbol{S}_1^{-1}. \tag{60}$$

From the above expression, we can see that, the first term in (60) is the CRLB for $\boldsymbol{\Phi}$ when the anchor timings and positions are accurate, and the second term represents the increase in CRLB of $\boldsymbol{\Phi}$ when there are uncertainties in the anchor timings and locations.

C. MSE Analysis for LS-I

The covariance matrix for the estimation of $\boldsymbol{\omega} = [x,\ y,\ \theta_1,\ \theta_2]^T$ in (26) can be derived as [22]

$$\boldsymbol{C}_{\mathrm{CWLS}} = \left(\hat{\boldsymbol{G}}_1^T \boldsymbol{C}_{\mathrm{WLS}}^{-1} \hat{\boldsymbol{G}}_1\right)^{-1} = \left(\hat{\boldsymbol{G}}_1^T \boldsymbol{A}^T \hat{\boldsymbol{C}}_e^{-1} \boldsymbol{A} \hat{\boldsymbol{G}}_1\right)^{-1}. \tag{61}$$

The variances of x, y, θ_1, and θ_2 are then given by the four diagonal elements of $\boldsymbol{C}_{\mathrm{CWLS}}$. In order to derive the variances of the original synchronization parameters θ_s and θ_0, note that θ_s and θ_0 are functions of θ_1 and θ_2 defined by

$$\theta_s = f_1(\theta_1) = \frac{1}{\theta_1}, \quad \theta_0 = f_2(\theta_1, \theta_2) = \frac{\theta_2}{\theta_1}. \tag{62}$$

Using the first-order Taylor series expansion, the Delta method [27] approximates the variances of θ_s and θ_0 by

$$\mathrm{var}(\theta_s)_{\mathrm{I}} = \left(\frac{df_1}{d\theta_1}\right)^2 \mathrm{var}(\theta_1)_{\mathrm{I}} = \frac{1}{\theta_1^4}\mathrm{var}(\theta_1)_{\mathrm{I}} \tag{63}$$

$$\mathrm{var}(\theta_0)_{\mathrm{I}} = \frac{\partial f_2}{\partial \boldsymbol{\theta}^T} \boldsymbol{C}_{\mathrm{I}} \frac{\partial f_2}{\partial \boldsymbol{\theta}} = \left[-\frac{\theta_2}{\theta_1^2}, \frac{1}{\theta_1}\right]^T \boldsymbol{C}_{\mathrm{I}} \left[-\frac{\theta_2}{\theta_1^2}, \frac{1}{\theta_1}\right] \tag{64}$$

where $\mathrm{var}(\theta_1)_{\mathrm{I}}$ (the third diagonal element of $\boldsymbol{C}_{\mathrm{CWLS}}$) is the estimation variance of θ_1 in LS-I, and $\boldsymbol{C}_{\mathrm{I}}$ is the covariance matrix of $\boldsymbol{\theta}$ in LS-I, which is the lower right 2×2 submatrix of $\boldsymbol{C}_{\mathrm{CWLS}}$.

When the LS-I algorithm is applied to the case with anchor uncertainties, the solution is given by (52) and the covariance matrix of the estimation of $\boldsymbol{\omega}$ is given by

$$\underline{\boldsymbol{C}}_{\mathrm{CWLS}} = \left(\underline{\boldsymbol{G}}_1^T \boldsymbol{H}^T \boldsymbol{C}_v^{-1} \boldsymbol{H} \underline{\boldsymbol{G}}_1\right)^{-1}. \tag{65}$$

The variances of x, y are given by the first two diagonal elements of $\underline{\boldsymbol{C}}_{\mathrm{CWLS}}$. The variances of θ_s and θ_0 are obtained similarly as in (63) and (64) but with $\mathrm{var}(\theta_1)_{\mathrm{I}}$ replaced by the third diagonal element of $\underline{\boldsymbol{C}}_{\mathrm{CWLS}}$ and $\boldsymbol{C}_{\mathrm{I}}$ replaced by the lower right 2×2 submatrix of $\underline{\boldsymbol{C}}_{\mathrm{CWLS}}$.

D. MSE Analysis for LS-II

The covariance matrix of the estimation of $\boldsymbol{\omega}$ in (51) is

$$\boldsymbol{C}_{\mathrm{CGTLS}} = \left(\hat{\boldsymbol{G}}_2^T \hat{\boldsymbol{C}}_{\mathrm{GTLS}}^{-1} \hat{\boldsymbol{G}}_2\right)^{-1} \tag{66}$$

and the variances of x, y, θ_1, and θ_2 are then given by the four diagonal elements of $\boldsymbol{C}_{\mathrm{CGTLS}}$. Similar to the derivations in the above subsection, the approximated variances of θ_s and θ_0 are

$$\mathrm{var}(\theta_s)_{\mathrm{II}} = \frac{1}{\theta_1^4}\mathrm{var}(\theta_1)_{\mathrm{II}} \tag{67}$$

$$\mathrm{var}(\theta_0)_{\mathrm{II}} = \left[-\frac{\theta_2}{\theta_1^2}, \frac{1}{\theta_1}\right]^T \boldsymbol{C}_{\mathrm{II}} \left[-\frac{\theta_2}{\theta_1^2}, \frac{1}{\theta_1}\right] \tag{68}$$

where $\mathrm{var}(\theta_1)_{\mathrm{II}}$ (the third diagonal element of $\boldsymbol{C}_{\mathrm{CGTLS}}$) is the estimation variance of θ_1 in LS-II and $\boldsymbol{C}_{\mathrm{II}}$ is the lower right 2×2 submatrix of $\boldsymbol{C}_{\mathrm{CGTLS}}$.

VI. Simulation Results and Discussions

In this section, simulation results are presented to verify the effectiveness of the proposed schemes. In the simulations, there are three anchors located at (5, −9), (19, 21), and (35, 3), with the unit of meter (m). The location of Node B is randomly generated from a square region with x and y randomly drawn from [0, 15] m. Notice that this region mostly lies outside of the triangle formed by the three anchors. The time skew is randomly drawn from [0.998, 1.002], and the time offset is randomly drawn from [1, 10] ns. The number of round of two-way message exchange is set to $M = 4$ unless stated otherwise. The TOA detection error n_{lm} and $\bar{n}_{lm}$ are independent and identically distributed (i.i.d.) Gaussian random variables with zero mean and variance σ_n^2 [14]. The MSEs of the location, time skew and time offset estimations are defined as $\mathbb{E}\{(x-\hat{x})^2+(y-\hat{y})^2\}$, $\mathbb{E}\{(\theta_s - \hat{\theta_s})^2\}$ and $\mathbb{E}\{(\theta_0 - \hat{\theta_0})^2\}$, respectively. All simulation results are average of 1000 independent runs.

A. With Accurate Anchors

The case when timings and locations of the anchors are all accurate is considered first. In Fig. 2, the MSEs of the ML estimator and the proposed LS-I estimator are plotted versus the TOA detection error variance. In addition, the CRLB, the analytical MSE of LS-I, and the localization performance of the separate time synchronization and localization approach are also shown. The separate approach is a combination of two recent techniques. More specifically, the two-way ranging (TWR) in IEEE 802.15.4a standard [21] is used for localization, and the Gaussian ML-like estimator (GMLLE) in [9] is used for time synchronization.

From Fig. 2, it can be seen that the separate approach only provides good estimates when $1/\sigma_n^2$ is small. However, when $1/\sigma_n^2$ is large, it reaches an error floor very quickly. Although the accuracy provided by the TWR may be sufficient in some applications, the joint approaches (ML and LS-I) follow the trend of the CRLB without incurring error floor. In particular, the ML estimation performance touches the CRLB. For LS-I, although it cannot reach the CRLB, the degradation is small. Furthermore, the analytical MSE expression derived for LS-I predicts the simulated performance very well. Fig. 3 shows the corresponding results of time skew and time offset estimations, illustrating that the ML is efficient. It can also be seen that, with accurate anchors, both LS-I and the separate approach have close to optimal timing estimation performances.

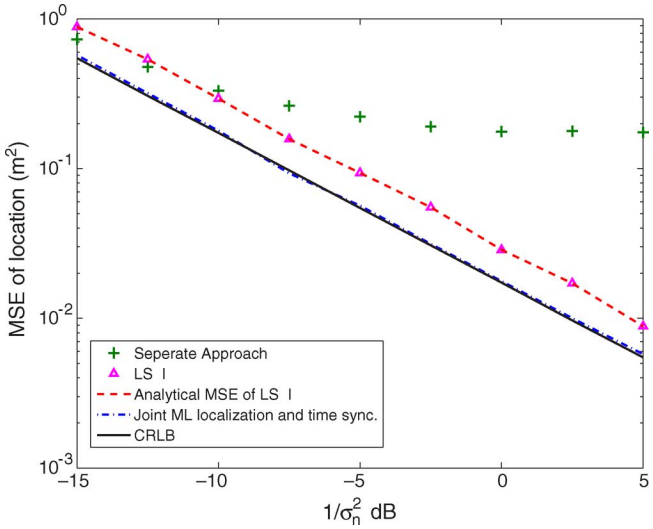

Fig. 2. MSE of location estimates versus TOA detection error variance $1/\sigma_n^2$, with accurate anchors.

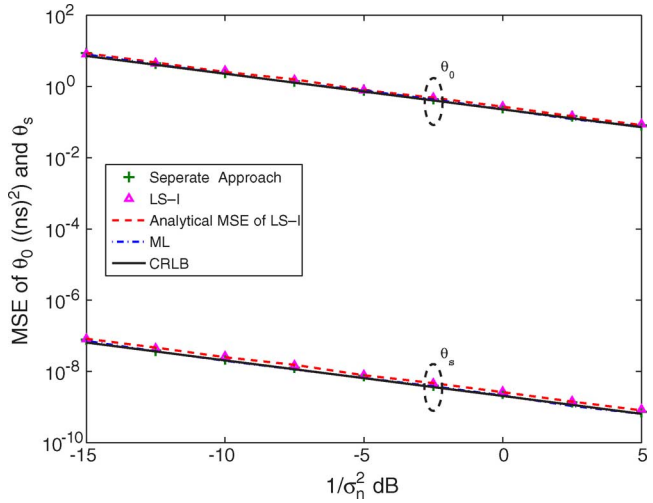

Fig. 3. MSE of θ_s and θ_0 estimates versus TOA detection error variance $1/\sigma_n^2$, with accurate anchors.

B. With Anchor Uncertainties

Figs. 4 and 5 show the CRLBs (under both accurate and inaccurate anchors) and the MSEs of various algorithms versus TOA detection error variance in the presence of anchor uncertainties. The variances of uncertainties in anchor locations, time skew and time offset are $1/\sigma_a^2 = 40$ dB, $1/\sigma_s^2 = 70$ dB, and $1/\sigma_0^2 = 20$ dB, respectively. For simplicity, we consider the case that uncertainties in anchor locations, time skews and time offsets are independent.

It can be seen that there are observable degradations in CRLBs when the anchors are inaccurate compared to the CRLBs with accurate anchors. For location estimation, the proposed LS-II provides more accurate estimation than LS-I and the separate approach especially when $1/\sigma_n^2$ is large, and the performance gap between LS-II and the CRLB is not significant. Furthermore, the performance of the proposed LS-II is well predicted by the analytical MSE expression. For timing estimation, LS-I and LS-II perform similarly and are close

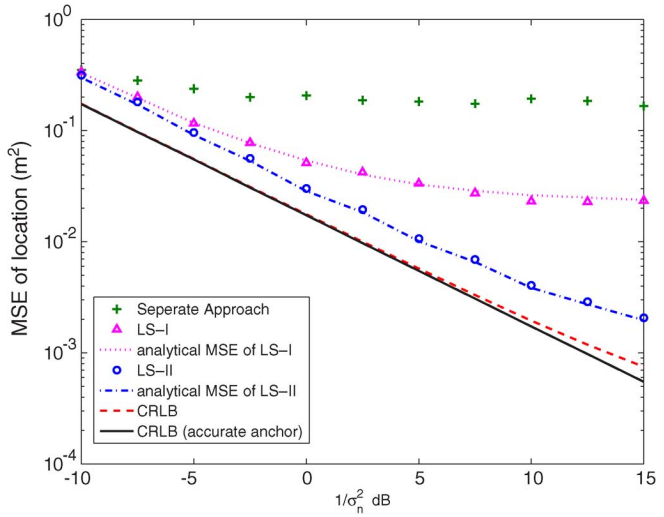

Fig. 4. MSE of location estimates versus TOA detection error variance $1/\sigma_n^2$, with anchor location error variance $1/\sigma_a^2 = 40$ dB, and anchor timing error variances $1/\sigma_s^2 = 70$ dB and $1/\sigma_0^2 = 20$ dB.

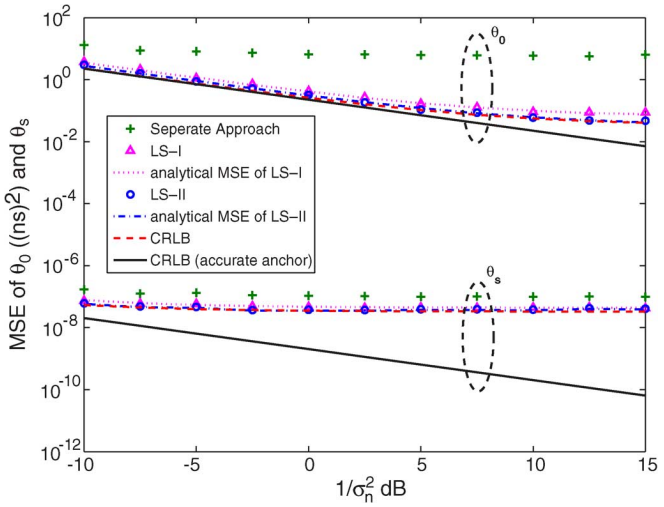

Fig. 5. MSE of θ_s and θ_0 estimates versus TOA detection error variance $1/\sigma_n^2$, with anchor location error variance $1/\sigma_a^2 = 40$ dB, and anchor timing error variances $1/\sigma_s^2 = 70$ dB and $1/\sigma_0^2 = 20$ dB.

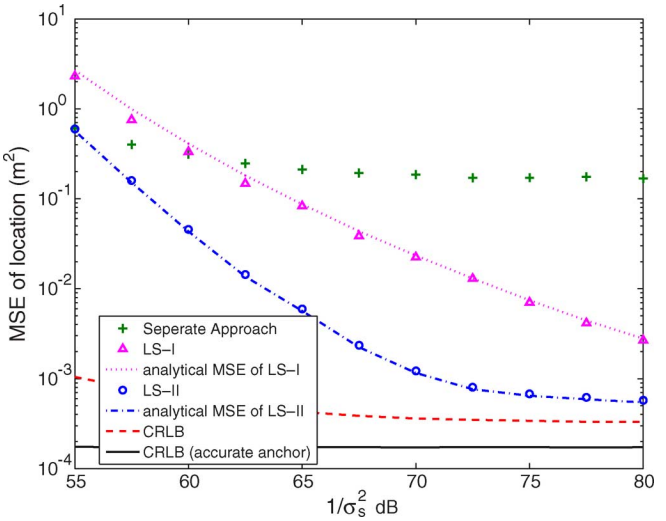

Fig. 6. MSE of location estimates versus anchor time skew uncertainty variance $1/\sigma_s^2$, with TOA detection error variance $1/\sigma_n^2 = 20$ dB, anchor location error variance $1/\sigma_a^2 = 40$ dB and anchor time offset error variance $1/\sigma_0^2 = 20$ dB.

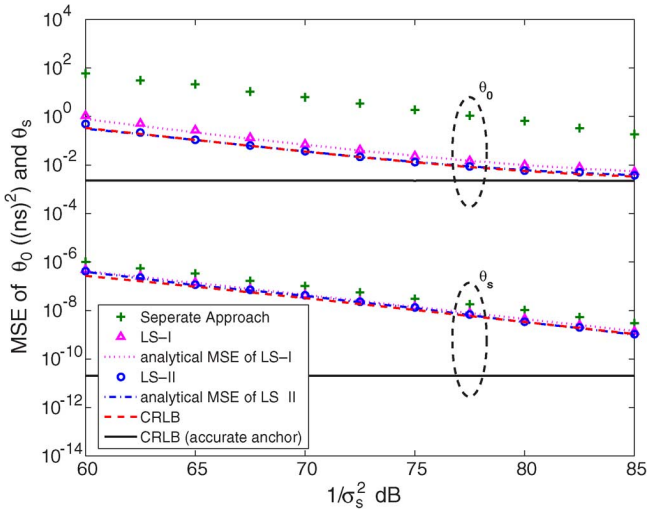

Fig. 7. MSE of θ_s and θ_0 estimates versus anchor time skew uncertainty variance $1/\sigma_s^2$, with TOA detection error variance $1/\sigma_n^2 = 20$ dB, anchor location error variance $1/\sigma_a^2 = 40$ dB and anchor time offset error variance $1/\sigma_0^2 = 20$ dB.

to optimal, while the separate approach suffers observable degradation.

Fig. 6 illustrates the location estimation performances of various algorithms as a function of time skew uncertainty, when variances of TOA detection error, uncertainties in anchor locations and time offset are $1/\sigma_n^2 = 20$ dB, $1/\sigma_a^2 = 40$ dB, and $1/\sigma_0^2 = 20$ dB, respectively. It is clear that when the time skew uncertainty σ_s decreases (i.e., $1/\sigma_s^2$ increases), the performances of LS-I and LS-II tends to converge to stable values not far from the CRLB with inaccurate anchor. However, the convergence speed of the LS-II is much faster than that of LS-I. On the other hand, the location estimation accuracy of separate approach does not improve much as the time skew uncertainty decreases.

With the same setting as in Fig. 6, Fig. 7 shows the corresponding performances for time skew and time offset estimation. It can be seen that LS-I and LS-II perform very close to CRLB. While the separate approach also follows the trend of CRLB, it shows a noticeable performance gap, especially in time offset estimation. When we vary the anchor location uncertainty variance $1/\sigma_a^2$ or time offset uncertainty variance $1/\sigma_0^2$ and evaluate the localization and synchronization performances of different algorithms, conclusions similar to those in Figs. 6 and 7 can be drawn. Therefore, the results are not repeated here.

Finally, the location and timing estimation performances of LS-I and LS-II versus the number of message-exchange round are illustrated in Figs. 8 and 9, respectively. These figures are generated with variances of TOA detection error, anchor location, anchor time skew and anchor time offset errors set to $1/\sigma_n^2 = 30$ dB, $1/\sigma_a^2 = 50$ dB, $1/\sigma_s^2 = 80$ dB, and $1/\sigma_0^2 = 20$ dB, respectively. It can be seen that as the number of message-exchange increases, both location and timing estimation

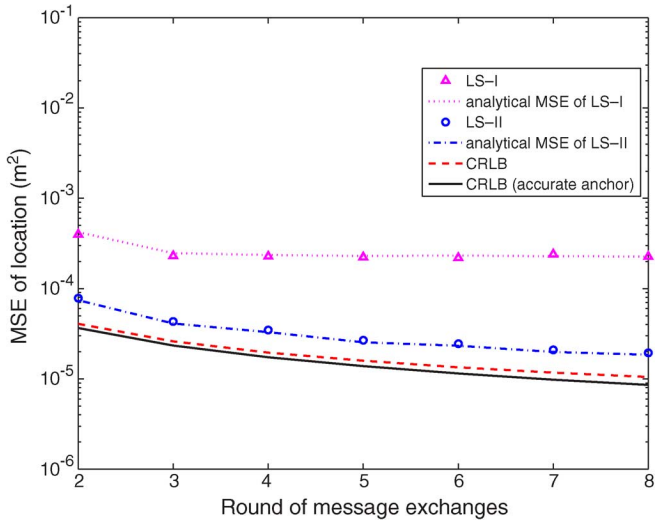

Fig. 8. MSE of location estimates versus number of message exchange round, with TOA detection error variance $1/\sigma_n^2 = 30$ dB, anchor location error variance $1/\sigma_a^2 = 50$ dB, anchor time skew error variance $1/\sigma_s^2 = 80$ dB, and anchor time offset error variance $1/\sigma_0^2 = 20$ dB.

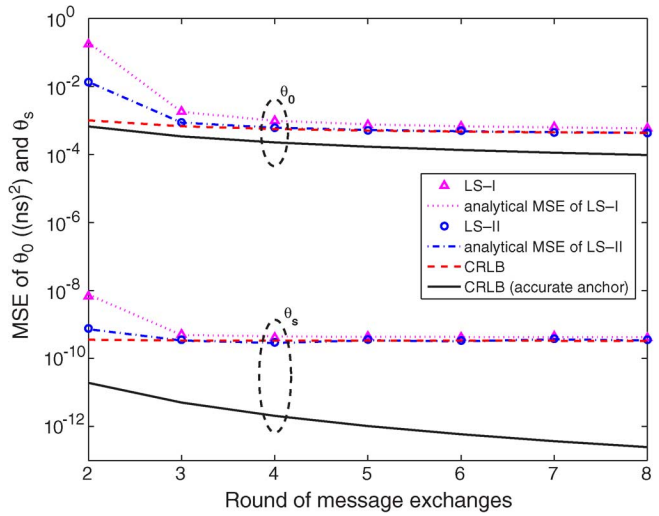

Fig. 9. MSE of timing estimates versus number of message exchange round, with TOA detection error variance $1/\sigma_n^2 = 30$ dB, anchor location error variance $1/\sigma_a^2 = 50$ dB, anchor time skew error variance $1/\sigma_s^2 = 80$ dB, and anchor time offset error variance $1/\sigma_0^2 = 20$ dB.

performances converge quickly to stable values. When more than four rounds of message exchanges are used, the estimation performance improvement is marginal.

VII. Conclusion

In this paper, a unified framework which jointly solves the time synchronization and localization problems in WSNs was proposed. We considered two cases in detail. In the first case, anchor locations and timings are assumed to be accurate. The maximum likelihood (ML) estimator was derived first. However, it is not in closed-form and therefore computationally expensive. Then, an efficient two-stage least squares based closed-form estimator (LS-I) was proposed. The second case we considered is when anchor timings and locations are not accurate. The system can be modeled as a linear equation with errors in the model matrix. A generalized total least squares based scheme (LS-II) was proposed to tackle the anchor uncertainties. Cramér–Rao lower bounds (CRLBs) and the analytical mean square error (MSE) expressions for the proposed LS-I and LS-II algorithms were also derived.

Results show that, in both cases with accurate anchors and with anchor uncertainties, the proposed joint time synchronization and localization approach outperforms the separate approach. The proposed LS-I and LS-II provide close to optimal performances in their respective scenarios. Furthermore, the performances are accurately predicted by their analytical MSE expressions.

Appendix
Derivation of $\boldsymbol{C}_v$ and $\boldsymbol{C}_U$

For notational simplicity, we define the following symbols. The errors in anchor timings and locations are grouped together and denoted as $\Delta\boldsymbol{k} = [\Delta a_{x1}, \Delta a_{y1}, \Delta\theta_{s1}, \Delta\theta_{01}, \cdots, \Delta a_{xL}, \Delta a_{yL}, \Delta\theta_{sL}, \Delta\theta_{0L}]^T$ with covariance matrix $\boldsymbol{C}_k$. The observed x coordinates, y coordinates, time skews and time offsets of anchors are $\boldsymbol{a}_x = [a_{x1}, \cdots, a_{xL}]^T$, $\boldsymbol{a}_y = [a_{y1}, \cdots, a_{yL}]^T$, $\boldsymbol{\theta}_s = [\theta_{s1}, \cdots, \theta_{sL}]^T$ and $\boldsymbol{\theta}_0 = [\theta_{01}, \cdots, \theta_{0L}]^T$ and their error vectors are denoted as $\Delta\boldsymbol{a}_x = [\Delta a_{x1}, \cdots, \Delta a_{xL}]^T$ with covariance matrix $\boldsymbol{C}_x$, $\Delta\boldsymbol{a}_y = [\Delta a_{y1}, \cdots, \Delta a_{yL}]^T$ with covariance matrix $\boldsymbol{C}_y$, $\Delta\boldsymbol{\theta}_s = [\Delta\theta_{s1}, \cdots, \Delta\theta_{sL}]^T$ with covariance matrix $\boldsymbol{C}_s$, and $\Delta\boldsymbol{\theta}_0 = [\Delta\theta_{01}, \cdots, \Delta\theta_{0L}]^T$ with covariance matrix $\boldsymbol{C}_o$, respectively. Moreover, the cross-correlation matrices between different error vectors are defined as $\boldsymbol{C}_{xy} = \mathbb{E}\{\boldsymbol{a}_x\boldsymbol{a}_y^T\}$, $\boldsymbol{C}_{xs} = \mathbb{E}\{\boldsymbol{a}_x\boldsymbol{\theta}_s^T\}$, $\boldsymbol{C}_{xo} = \mathbb{E}\{\boldsymbol{a}_x\boldsymbol{\theta}_o^T\}$, $\boldsymbol{C}_{ys} = \mathbb{E}\{\boldsymbol{a}_y\boldsymbol{\theta}_s^T\}$, and $\boldsymbol{C}_{ys} = \mathbb{E}\{\boldsymbol{a}_y\boldsymbol{\theta}_o^T\}$. The covariance matrix of each measured anchor location vector is defined as $\boldsymbol{C}_{ai} = \mathbb{E}\{\boldsymbol{a}_i\boldsymbol{a}_i^T\}$. Note that elements of $\boldsymbol{C}_{xy}$, $\boldsymbol{C}_x$, $\boldsymbol{C}_y$, $\boldsymbol{C}_s$, $\boldsymbol{C}_o$, $\boldsymbol{C}_{xs}$, $\boldsymbol{C}_{xo}$, $\boldsymbol{C}_{ys}$, $\boldsymbol{C}_{yo}$ and $\boldsymbol{C}_{ai}$ can be determined from $\boldsymbol{C}_k$. Furthermore, we also define $\bar{\boldsymbol{\theta}}_s \triangleq [1/\theta_{s1}, \cdots, 1/\theta_{sL}]^T$.

Derivation of $\boldsymbol{C}_v$: Recalling the definition of $\boldsymbol{e}'$ in (39) and ignoring the second-order errors, $\boldsymbol{e}'$ can be represented as

$$\boldsymbol{e}' = 2\boldsymbol{T}_e' \odot [\boldsymbol{n} + \boldsymbol{T}_1 \odot (\Delta\boldsymbol{\theta}_s \otimes \boldsymbol{1}_{2M\times 1}) - \boldsymbol{T}_2 \odot (\Delta\boldsymbol{\theta}_0 \otimes \boldsymbol{1}_{2M\times 1})] \quad (69)$$

where

$$\boldsymbol{T}_e' = \boldsymbol{T}_b\theta_1 - \theta_2\boldsymbol{E}_{2LM\times 1} - \boldsymbol{T}_a \odot [\bar{\boldsymbol{\theta}}_s \otimes \boldsymbol{1}_{2M\times 1}] + (\boldsymbol{\theta}_0 \odot \bar{\boldsymbol{\theta}}_s) \otimes \boldsymbol{E}_{2M\times 1}, \quad (70)$$

$$\boldsymbol{T}_1 = -\boldsymbol{T}_a \odot \left[(\bar{\boldsymbol{\theta}}_s \odot \bar{\boldsymbol{\theta}}_s) \otimes \boldsymbol{1}_{2M\times 1}\right] + (\bar{\boldsymbol{\theta}}_s \odot \bar{\boldsymbol{\theta}}_s) \otimes \boldsymbol{E}_{2M\times 1}, \quad (71)$$

$$\boldsymbol{T}_2 = \bar{\boldsymbol{\theta}}_s \otimes \boldsymbol{E}_{2M\times 1}, \quad (72)$$

and $\boldsymbol{T}_a$ and $\boldsymbol{T}_b$ were introduced in (10). Similarly, $\Delta\boldsymbol{b}$ in (38) can be represented as

$$\Delta\boldsymbol{b} = \frac{2}{c^2}\left[\bar{\boldsymbol{a}}_x \odot (\Delta\boldsymbol{a}_x \otimes \boldsymbol{1}_{2M\times 1}) + \bar{\boldsymbol{a}}_y \odot (\Delta\boldsymbol{a}_y \otimes \boldsymbol{1}_{2M\times 1})\right] \quad (73)$$

where $\bar{\boldsymbol{a}}_x = \boldsymbol{a}_x \otimes \boldsymbol{1}_{2M\times 1}$ and $\bar{\boldsymbol{a}}_y = \boldsymbol{a}_y \otimes \boldsymbol{1}_{2M\times 1}$.

The covariance matrix of $\boldsymbol{v} = \Delta\boldsymbol{b} + \boldsymbol{e}'$ is given by

$$\begin{aligned}\boldsymbol{C}_v &= \mathbb{E}\{\boldsymbol{v}\boldsymbol{v}^T\} = \mathbb{E}\{\Delta\boldsymbol{b}\Delta\boldsymbol{b}^T\} + \mathbb{E}\{\boldsymbol{e}'\boldsymbol{e}'^T\} + 2\mathbb{E}\{\Delta\boldsymbol{b}\boldsymbol{e}'^T\} \\ &\triangleq \boldsymbol{C}_b + \boldsymbol{C}_{e'} + 2\boldsymbol{C}_{be'} \end{aligned} \tag{74}$$

where

$$\begin{aligned}\boldsymbol{C}_b &= \mathbb{E}\{\Delta\boldsymbol{b}\Delta\boldsymbol{b}^T\} \\ &= \frac{4}{c^4}\left[\left(\boldsymbol{a}_x\boldsymbol{a}_x^T\right)\odot\boldsymbol{C}_x + \left(\boldsymbol{a}_y\boldsymbol{a}_y^T\right)\odot\boldsymbol{C}_y + 2\left(\boldsymbol{a}_x\boldsymbol{a}_y^T\right)\odot\boldsymbol{C}_{xy}\right] \\ &\quad \otimes \mathbf{1}_{2M\times 2M} \end{aligned} \tag{75}$$

$$\begin{aligned}\boldsymbol{C}_{e'} &= \mathbb{E}\{\boldsymbol{e}'\boldsymbol{e}'^T\} \\ &= 4\left(\boldsymbol{T}'_e\boldsymbol{T}'^T_e\right) \\ &\quad \odot \Big[\boldsymbol{C}_n + \left(\boldsymbol{T}_1\boldsymbol{T}_1^T\right)\odot(\boldsymbol{C}_s\otimes\mathbf{1}_{2M\times 2M}) \qquad (76) \\ &\qquad + \left(\boldsymbol{T}_2\boldsymbol{T}_2^T\right)\odot(\boldsymbol{C}_o\otimes\mathbf{1}_{2M\times 2M}) \\ &\qquad + 2\left(\boldsymbol{T}_1\boldsymbol{T}_2^T\right)\odot(\boldsymbol{C}_{so}\otimes\mathbf{1}_{2M\times 2M})\Big] \qquad (77)\end{aligned}$$

$$\begin{aligned}\boldsymbol{C}_{be'} &= \mathbb{E}\{\Delta\boldsymbol{b}\boldsymbol{e}'^T\} \\ &= \frac{4}{c^2}\left(\mathbf{1}_{2LM\times 1}\boldsymbol{T}'^T_e\right) \\ &\quad \odot \Big[\left(\bar{\boldsymbol{a}}_x\boldsymbol{T}_1^T\right)\odot(\boldsymbol{C}_{xs}\otimes\mathbf{1}_{2M\times 2M}) \\ &\qquad - \left(\bar{\boldsymbol{a}}_x\boldsymbol{T}_2^T\right)\odot(\boldsymbol{C}_{xo}\otimes\mathbf{1}_{2M\times 2M}) \\ &\qquad + \left(\bar{\boldsymbol{a}}_y\boldsymbol{T}_1^T\right)\odot(\boldsymbol{C}_{ys}\otimes\mathbf{1}_{2M\times 2M}) \\ &\qquad - \left(\bar{\boldsymbol{a}}_y\boldsymbol{T}_2^T\right)\odot(\boldsymbol{C}_{yo}\otimes\mathbf{1}_{2M\times 2M})\Big]. \end{aligned} \tag{78}$$

Derivation of $\boldsymbol{C}_U$: It is assumed that the TOA detection error $\boldsymbol{n}$ is uncorrelated to the anchor timing and location error $\Delta\boldsymbol{k}$, because the errors are from different sources. Therefore, the covariance matrix of $\boldsymbol{U}^T$ is

$$\begin{aligned}\boldsymbol{C}_U &= \mathbb{E}\{\boldsymbol{U}^T\boldsymbol{U}\} = \begin{bmatrix}\mathbb{E}\{\delta\boldsymbol{A}^T\delta\boldsymbol{A}\} & \mathbb{E}\{\delta\boldsymbol{A}^T\boldsymbol{v}\} \\ \mathbb{E}\{\boldsymbol{v}^T\delta\boldsymbol{A}\} & \mathbb{E}\{\boldsymbol{v}^T\boldsymbol{v}\}\end{bmatrix} \\ &\triangleq \begin{bmatrix}\boldsymbol{C}_A & \boldsymbol{c}_{Av} \\ \boldsymbol{c}_{Av}^T & c_v\end{bmatrix}. \end{aligned} \tag{79}$$

Recall the definitions of $\delta\boldsymbol{A}$ and $\Delta\boldsymbol{b}$ in (37) and (38), and with $\boldsymbol{v} = \Delta\boldsymbol{b} + \boldsymbol{e}'$, the items in (79) can be shown to be

$$\boldsymbol{C}_A = \mathbb{E}\{\delta\boldsymbol{A}^T\delta\boldsymbol{A}\} = \frac{8M}{c^4}\sum_{i=1}^{L}\boldsymbol{C}_{ai} \tag{80}$$

$$\begin{aligned}\boldsymbol{c}_{Av} &= \mathbb{E}\{\delta\boldsymbol{A}^T\Delta\boldsymbol{b} + \delta\boldsymbol{A}^T\boldsymbol{e}'\} \\ &= \frac{8M}{c^4}\sum_{i=1}^{L}\boldsymbol{C}_{ai}\boldsymbol{a}_i + [\mathrm{Tr}(\boldsymbol{C}_{xe'}), \mathrm{Tr}(\boldsymbol{C}_{ye'})]^T \end{aligned} \tag{81}$$

$$c_v = \mathrm{Tr}(\boldsymbol{C}_v) \tag{82}$$

where

$$\begin{aligned}\boldsymbol{C}_{xe'} &= \mathbb{E}\left\{(\Delta\boldsymbol{a}_x\otimes\mathbf{1}_{2M\times 1})\boldsymbol{e}'^T\right\} \\ &= \frac{4}{c^2}\left(\mathbf{1}_{2LM\times 1}\boldsymbol{T}'^T_e\right) \\ &\quad \odot \Big[\left(\mathbf{1}_{2LM\times 1}\boldsymbol{T}_1^T\right)\odot(\boldsymbol{C}_{xs}\otimes\mathbf{1}_{2M\times 2M}) \\ &\qquad - \left(\mathbf{1}_{2LM\times 1}\boldsymbol{T}_2^T\right)\odot(\boldsymbol{C}_{xo}\otimes\mathbf{1}_{2M\times 2M})\Big] \end{aligned} \tag{83}$$

$$\begin{aligned}\boldsymbol{C}_{ye'} &= \mathbb{E}\left\{(\Delta\boldsymbol{a}_y\otimes\mathbf{1}_{2M\times 1})\boldsymbol{e}'^T\right\} \\ &= \frac{4}{c^2}\left(\mathbf{1}_{2LM\times 1}\boldsymbol{T}'^T_e\right) \\ &\quad \odot \Big[\left(\mathbf{1}_{2LM\times 1}\boldsymbol{T}_1^T\right)\odot(\boldsymbol{C}_{ys}\otimes\mathbf{1}_{2M\times 2M}) \\ &\qquad - \left(\mathbf{1}_{2LM\times 1}\boldsymbol{T}_2^T\right)\odot(\boldsymbol{C}_{yo}\otimes\mathbf{1}_{2M\times 2M})\Big]. \end{aligned} \tag{84}$$

REFERENCES

[1] *Secure Localization and Time Synchronization for Wireless Sensor and ad hoc Networks*, R. Poovendran, C. Wang, and S. Roy, Eds.. New York: Springer, 2006.

[2] *Wireless Sensor Networks: Signal Processing and Communications Perspective*, A. Swami, Q. Zhao, Y. Hong, and L. Tong, Eds.. New York: Wiley, 2007.

[3] N. Patwari, A. O. Hero, III, J. Ash, R. L. Moses, S. Kyperountas, and N. S. Correal, "Locating the nodes: Cooperative localization in wireless sensor networks," *IEEE Signal Process. Mag.*, vol. 22, no. 4, pp. 54–69, Jul. 2005.

[4] A. H. Sayed, A. Tarighat, and N. Khajehnouri, "Network-based wireless location: Challenges faced in developing techniques for accurate wireless location information," *IEEE Signal Process. Mag.*, vol. 22, no. 4, pp. 24–40, Jul. 2005.

[5] G. Mao, B. Fidan, and B. Anderson, "Wireless sensor network localization techniques," *Comput. Netw.*, vol. 51, no. 10, pp. 2529–2553, Jul. 2007.

[6] J. Elson, L. Girod, and D. Estrin, "Fine-grained network time synchronization using reference broadcasts," in *Proc. 5th Symp. on Operating Syst. Design and Implementation*, Boston, MA, Dec. 2002, pp. 147–163.

[7] S. Ganeriwal, R. Kumar, and M. B. Srivastava, "Timing-syn protocol for sensor networks," in *Proc. SenSys 03*, Los Angeles, CA, Nov. 2003, pp. 138–149.

[8] M. Maroti, B. Kusy, G. Simon, and A. Ledeczi, "The flooding time synchronization protocol," in *Proc. SenSys 04*, Baltimore, MD, Nov. 2004, pp. 39–49.

[9] K. Noh, Q. M. Chaudhari, E. Serpedin, and B. W. Suter, "Novel clock phase offset and skew estimation using two-way timing message exchanges for wireless sensor networks," *IEEE Trans. Commun.*, vol. 55, no. 4, pp. 766–777, 2007.

[10] B. Sundararaman, U. Buy, and A. Kshemkalyani, "Clock synchronization for wireless sensor networks: A survey," *Ad Hoc Netw.*, vol. 3, no. 3, pp. 281–323, May 2005.

[11] N. Priyantha, A. Chakraborty, and H. Balakrishnan, "The cricket location-support system," in *Proc. 6th Annu. ACM Int. Conf. Mobile Computing and Networking*, Aug. 2000, pp. 32–43.

[12] K. Romer and F. Mattern, "Towards a unified view on space and time in sensor networks," *Comput. Commun.*, vol. 28, pp. 1484–1497, Aug. 2005.

[13] H. Oliveira, E. Nakamura, and A. Loureiro, "Localization in time and space for sensor networks," in *Proc. 21st Int. Conf. Adv. Inf. Net. Appl.*, May 2007, pp. 539–546.

[14] B. Denis, J. Pierrot, and C. Abou-Rjeily, "Joint distributed synchronization and positioning in UWB *ad hoc* networks using ToA," *IEEE Trans. Microw. Theory Tech.*, vol. 54, no. 4, pp. 1896–1911, Jun. 2006.

[15] A. Savvides, C.-C. Han, and M. B. Strivastava, "Dynamic fine-grained localization in ad hoc networks of sensors," in *Proc. 7th Annu. Int. Conf. Mobile Comput. Netw. (MobiCom) 2001*, Jul. 2001, pp. 166–179.

[16] K. C. Ho, X. Lu, and L. Kovavisaruch, "Source localization using TDOA and FDOA measurements in the presence of receiver location errors: Analysis and solution," *IEEE Trans. Signal Process.*, vol. 55, no. 2, pp. 684–696, Feb. 2007.

[17] N. Marechal, J. Peerrot, and J. Gorce, "Fine synchronization for wireless sensor networks using gossip averaging algorithms," presented at the Int. Conf. Commun. (ICC), Beijing, May 2008.

[18] K. Iwanicki, M. Steen, and S. Voulgaris, "Gossip-based clock synchronization for large decentralized systems," in *Proc. 2nd IEEE Int. Workshop Self-Managed Netw., Syst., Services*, 2006.

[19] I. Wokoma, I. Liabotis, O. Prnjat, L. Sacks, and I. Marshall, "A weakly coupled adaptive gossip protocol for application level active networks," in *Proc. 3rd Int. Workshop Policies Distribut. Syst. Netw.*, 2002.

[20] N. Freris and P. Kumar, "Fundamental limits on synchronization of affine clocks in networks," in *46th IEEE Conf. Decision Control*, Dec. 2007.

[21] *Annex D1: Location Topics*, IEEE Standard 802.15.4a, Aug. 2007.
[22] S. Kay, *Fundamentals of Statistical Signal Processing: Estimation Theory*. Englewood Cliffs, NJ: Prentice-Hall, 1993.
[23] I. Ziskind and M. Wax, "Maximum likelihood localization of multiple sources by alternating projection," *IEEE Trans. Signal Process.*, vol. 36, no. 10, pp. 1553–1560, Oct. 1998.
[24] S. Van Huffel and J. Vandewalle, *The Total Least-Squares Problem: Computational Aspects and Analysis*. Philadelphia, PA: SIAM, 1991, vol. 9, Frontier in Applied Mathematics.
[25] S. Van Huffel and J. Vandewalle, "Analysis and properties of the generalized total least squares problem $AX \approx B$ when some or all columns in A are subject to error," *SIAM J. Matrix Anal. Appl.*, vol. 10, no. 3, pp. 294–315, Jul. 1989.
[26] P. Stoica and K. Sharman, "Maximum likelihood methods for direction of arrival estimation," *IEEE Trans. Acoust., Speech, Signal Process.*, vol. 38, pp. 1132–1143, Jul. 1990.
[27] H. K. Tiwari and R. C. Elston, "The approximate variance of a function of random variables," *Biometrical J.*, vol. 41, no. 3, pp. 351–357, 1999.

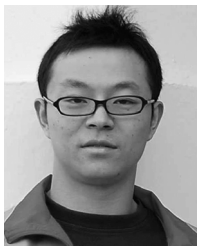

Jun Zheng received the B.Eng. degree from the University of Electronic Science and Technology of China in 2005 and the M.Phil. degree from the University of Hong Kong in 2009.

From 2006 to 2007, he was a Research Assistant at the City University of Hong Kong and then at the Hong Kong University of Science and Technology. He is currently working towards the Ph.D. degree at the University of Texas—Austin. His research interests are statistical signal processing, communication systems, and machine learning.

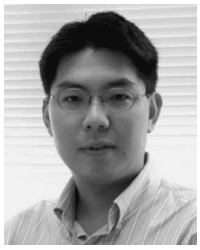

Yik-Chung Wu received the B.Eng. degree in electrical and electronic engineering and the M.Phil. degree both from the University of Hong Kong (HKU) in 1998 and 2001, respectively, and the Ph.D. degree from Texas A&M University, in 2005.

After graduating from Master's studies, he was a Research Assistant at the University of Hong Kong. From August 2005 to August 2006, he was a Member of Technical Staff with the Thomson Corporate Research, Princeton, NJ. Since September 2006, he has been with the University of Hong Kong as an Assistant Professor. His research interests are in the general area of signal processing and communication systems, and in particular receiver algorithm design, synchronization techniques, channel estimation, and equalization.

During his study at Texas A&M University, Dr. Wu was fully supported by the prestigious Croucher Foundation scholarship. He was a TPC member for IEEE VTC Fall 2005, IEEE GLOBECOM 2006 and 2008, and ICC 2007 and 2008. He is currently serving as an Associate Editor for the IEEE COMMUNICATIONS LETTERS.